CHEMISTRY
A EUROPEAN JOURNAL

DOI: 10.1002/chem.200600615

VIP

A Synthetic Breakthrough into an Unanticipated Stability Regime: A Series of Isolable Complexes in which C_6, C_8, C_{10}, C_{12}, C_{16}, C_{20}, C_{24}, and C_{28} Polyynediyl Chains Span Two Platinum Atoms

Qinglin Zheng,[a] James C. Bohling,[b] Thomas B. Peters,[b] Anja C. Frisch,[a] Frank Hampel,[a] and J. A. Gladysz*[a]

Abstract: The reaction of *trans*-[PtCl(*p*-tol){P(*p*-tol)$_3$}$_2$] (**PtCl**) and H(C≡C)$_2$H (cat. CuI, HNEt$_2$) gives **PtC$_4$H** (82%), which can be cross-coupled with excess HC≡CSiEt$_3$ (acetone, O$_2$, CuCl/TMEDA; Hay conditions) to yield **PtC$_6$Si** (77%). The addition of nBu$_4$N$^+$F$^-$ in wet acetone gives **PtC$_6$H** (84%), and further addition of ClSiMe$_3$ (F$^-$ scavenger) and excess HC≡CSiEt$_3$ (Hay conditions) yields **PtC$_8$Si** (23%). Similar cross-coupling reactions of **PtC$_x$H** (generated in situ for $x>6$) and excess H(C≡C)$_2$SiEt$_3$ give a) $x=4$, **PtC$_8$Si** (29%), **PtC$_{12}$Si** (30%), and **PtC$_{16}$Si** (1%); b) $x=6$, **PtC$_{10}$Si** (59%) and **PtC$_{14}$Si** (7%); c) $x=8$, **PtC$_{12}$Si** (42%); and d) $x=10$, **PtC$_{14}$Si** (20%). Hay homocoupling reactions of **PtC$_4$H**, **PtC$_6$H**, **PtC$_8$H**, and **PtC$_{10}$H** give **PtC$_8$Pt**, **PtC$_{12}$Pt**, **PtC$_{16}$Pt**, and **PtC$_{20}$Pt** (88–70%), but **PtC$_{12}$H** decomposes too rapidly. However, when **PtC$_{12}$Si** and **PtC$_{14}$Si** are subjected to Hay conditions, protodesilylation occurs in the presence of the oxidizing agent and **PtC$_{24}$Pt** (36%) and **PtC$_{28}$Pt** (51%) are isolated. Reactions of **PtC$_6$H** and **PtC$_{10}$H** with **PtCl** (CuI, HNEt$_2$) give **PtC$_6$Pt** (56%) and **PtC$_{10}$Pt** (84%). The effect of the chain lengths in **PtC$_x$Pt** upon thermal stabilities (>200 °C for $x\leq 20$), IR $\nu_{C\equiv C}$ patterns (progressively more bands), colors (yellow to orange to deep red), UV/Vis spectra (progressively red-shifted and more intense bands with $\varepsilon > 400\,000\,M^{-1}cm^{-1}$), redox properties (progressively more difficult oxidations), and NMR spectra (many monotonic trends) are analyzed, including implications for the sp carbon allotrope carbyne. Whereas all other dodecaynes and tetradecaynes rapidly decompose at room temperature, **PtC$_{24}$Pt** and **PtC$_{28}$Pt** remain stable at >140 °C. Crystal structures of **PtC$_x$Si** ($x=6$, 8, 10) and **PtC$_x$Pt** ($x=6$, 8, 10, 12) have been determined.

Keywords: carbyne · oxidative coupling · platinum · polyynes · structure elucidation · UV/Vis spectroscopy

Introduction

Chains of sp carbon atoms (C_x chains) represent the most basic and wirelike unsaturated bridging organic ligands, and they are impossible to twist out of conjugation. Accordingly, they are used extensively as connecting units in sophisticated molecular assemblies.[1] Two decades ago, only a handful of compounds were known in which such moieties spanned two transition metals, $[(L)_mMC_xM'(L')_{m'}]$.[2] There are now numerous examples,[2–4] the result of extensive efforts that have been motivated by a variety of fundamental and applied objectives. Many of the latter are connected to redox and charge- or energy-transfer phenomena involving the metal termini.[2,3,5]

Early studies often focused on the breadth of complexes that can be made. However, many current efforts seek to test the limits of homologous series of compounds. One

[a] Q. Zheng, Dr. A. C. Frisch, Dr. F. Hampel, Prof. Dr. J. A. Gladysz
Institut für Organische Chemie
Friedrich-Alexander-Universität Erlangen-Nürnberg
Henkestrasse 42, 91054 Erlangen (Germany)
Fax: (+49) 9131-852-6865
E-mail: gladysz@organik.uni-erlangen.de

[b] Dr. J. C. Bohling, Dr. T. B. Peters
Department of Chemistry, University of Utah
Salt Lake City, UT 84112 (USA)

Supporting information for this article is available on the WWW under http://www.chemeurj.org/ or from the author. It contains fifteen figures illustrating CV traces for **PtC$_x$Pt**, graphical analyses of NMR data, and packing diagrams for crystallographically characterized compounds.

thrust has involved extremes in oxidation states—that is, how many can be generated, or how far a complex can be oxidized or reduced—and the consequences for electronic and geometric structure, and reactivity.[3,6] Another thrust has involved extremes in chain lengths. Are there practical upper limits, and do the challenges have more to do with synthetic methodologies or product stabilities? The longer the chains, the closer the complexes model the polymeric sp carbon allotrope, carbyne.[7] Despite many studies, this remains the poorest characterized and understood of the classical carbon allotropes.

Most homologous series of C_x complexes characterized to date have polyynediyl structures, $[(L)_mM(C{\equiv}C)_nM(L)_m]$. Species with cumulenic bridges are much less stable.[8] Of the polyynediyl complexes, only those with $\{Fe(\eta^5\text{-}C_5Me_5)(CO)_2\}$,[9] $\{Ru(\eta^5\text{-}C_5R_5)(L)_2\}$ or $\{Ru(L')(L)_4\}^{n+}$,[10] $\{Re(\eta^5\text{-}C_5Me_5)(NO)(PPh_3)\}$,[11] $\{Ru_2(2\text{-anilinopyridinate})_4\}$,[12] $\{Pt(C_6F_5)\{P(p\text{-tol})_3\}_2\}$,[13] and $\{Pt(C_6F_5)(RAr_2P)_2\}$[14] endgroups have been extended to long chain lengths, *beyond* four triple bonds ($\geq C_{10}$). Interesting related complexes with tricobalt clusters joined by $\mu_3\text{-}\eta^1$-carbon chains have also been reported.[10a] However, it has so far only proved possible to isolate significant quantities of one eicosadecaynediyl or C_{20} complex, which has $\{Re(\eta^5\text{-}C_5Me_5)(NO)(PPh_3)\}$ endgroups.[11a] Outside of trace quantities evidenced by HPLC and UV/Vis spectra,[13] other C_{20} or higher species have remained unknown.

In this paper, we describe the most extensive series of C_x complexes isolated to date ($x = 6$, 8, 10, 12, 16, 20, 24, 28) and their detailed physical characterization. These feature the *p*-tolyl-substituted platinum endgroup $\{Pt(p\text{-tol})\{P(p\text{-tol})_3\}_2\}$, which is more electron-rich than the pentafluorophenyl analogue mentioned above.[13] Complexes in this series are designated **PtC$_x$Pt**, per the nomenclature system exemplified in Scheme 1. The two highest members, **PtC$_{24}$Pt** and **PtC$_{28}$Pt**, were isolated by a new coupling protocol that may have considerable generality. The effect of chain length upon thermal, spectroscopic, redox, and structural properties is carefully documented. These data help, together with those for all series of C_x complexes, to bound the properties of the polymeric sp carbon allotrope carbyne.[7] A portion of this work has been communicated.[15]

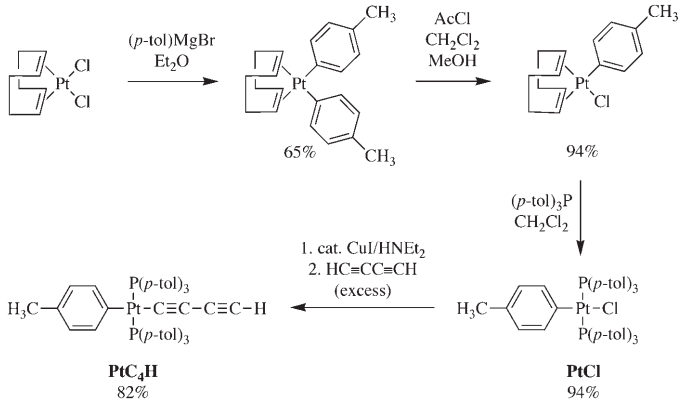

Scheme 1. Synthesis of precursor complexes.

Results

Syntheses of monoplatinum complexes: Platinum chloride complexes are easily converted to butadiynyl complexes,[13,14a,16] which are versatile platforms for sp carbon chain extension. Thus, a route to *trans*-$[PtCl(p\text{-tol})\{P(p\text{-tol})_3\}_2]$ (**PtCl**) was sought. The cyclooctadiene (cod) complex $[PtCl_2(cod)]$, which is readily available from K_2PtCl_4,[17] was treated with the commercial Grignard reagent *p*-tolMgBr (2.5 equiv). As shown in Scheme 1, workup gave the bis(*p*-tolyl) complex $[Pt(cod)(p\text{-tol})_2]$ in 65% yield.[18] Subsequent treatment with HCl, generated from acetyl chloride (1.7 equiv) in $MeOH/CH_2Cl_2$, afforded the chloride complex $[PtCl(p\text{-tol})(cod)]$ (94%).[19] Reaction with $P(p\text{-tol})_3$ then gave the target molecule **PtCl** (94%). As with all bis(phosphine) complexes below, NMR spectra showed virtual coupling.[20] In this case, the ^{13}C NMR signal for the ipso carbon atoms of the $P(p\text{-tol})_3$ groups was a triplet, with equal apparent coupling to both phosphorus atoms.

In accord with literature precedent,[13,14a,16] a solution of **PtCl** and CuI (0.12 equiv) in $HNEt_2$ was treated with excess $H(C{\equiv}C)_2H$[21] in THF. As shown in Scheme 1, workup gave the butadiynyl complex *trans*-$[Pt(p\text{-tol})\{P(p\text{-tol})_3\}_2\{(C{\equiv}C)_2H\}]$ (**PtC$_4$H**) as a tan powder in 82% yield. All new complexes that could be isolated in sufficient quantity were characterized by IR, NMR (^1H, ^{13}C, ^{31}P), and UV/Vis spectroscopy, as well as mass spectrometry, microanalysis, DSC, and TGA. Key data are summarized in Tables 1–4, and are analyzed below. Other data are supplied in the Experimental Section. In the case of **PtC$_4$H**, the butadiynyl ^{13}C NMR signals exhibited coupling constant patterns (J(C,H), J(C,Pt), J(C,P)) that allowed unambiguous assignments (Table 3 and Experimental Section). These facilitate signal assignments with the longer chain complexes.

We next sought to extend the sp carbon chain in **PtC$_4$H** by means of oxidative cross coupling reactions. To prepare as many homologues as possible, initial efforts used the commercially available two-carbon building block, $HC{\equiv}CSiEt_3$. Hay conditions (excess O_2, cat. CuCl/TMEDA, acetone)[22] are often effective with platinum alkynyl complexes (TMEDA = *N*,*N*,*N*′,*N*′-tetramethyl-1,2-ethanediamine). Thus, as shown in Scheme 2, **PtC$_4$H** and a 30-fold excess of $HC{\equiv}CSiEt_3$ were similarly condensed. Workup gave the yellow triethylsilylhexatriynyl complex **PtC$_6$Si** in 77% yield. When 20- or 10-fold excesses were employed, yields were lower. The coupling proceeds under milder conditions than with the analogous pentafluorophenyl platinum complex.[13] Presumably the more electron releasing *p*-tolyl ligand facilitates oxidation.

To further extend the sp carbon chain, the protodesilylation of **PtC$_6$Si** was attempted. As shown in Scheme 2, the addition of $n Bu_4N^+F^-$ in wet THF gave the hexatriynyl complex **PtC$_6$H** in 84% yield after a low-temperature

Table 1. Thermal stability data [°C].

	Mass loss (onset) TGA	DSC $T_i/T_e/T_p/T_c/T_f$	Decomposition (onset) capillary thermolysis[a]
PtC_4H	192	179/–/–/–/–[b]	180[c]
PtC_6Si	220	221/232/234/235/235[d]	220[e]
PtC_8Si	214	127/137/147/154/162[d]	
		184/–/–/–/–[b]	112[e]
$PtC_{10}Si$	233	128/140/146/150/162[b]	
		204/216/221/229/239[b]	105[f]
$PtC_{12}Si$	240	143/167/186/200/209[b]	101[f]
$PtC_{14}Si$	253	126/140/157/169/182[b]	
		186/186/193/197/198[b]	
		204/216/221/229/239[b]	105[f]
$PtC_{16}Si$	–	–	104[f]
PtC_6Pt	221	134/138/144/148/155[b]	
		199/–/–/–/–[b]	204[f]
PtC_8Pt	221	140/152/165/178/188[b]	
		190/194/203/211/214[b]	206[f]
$PtC_{10}Pt$	238	223/–/–/–/–[b]	230[f]
$PtC_{12}Pt$	228	250/–/–/–/–[b]	245[f]
$PtC_{16}Pt$	237	199/–/–/–/–[b]	200[f]
$PtC_{20}Pt$	222	142/152/168/185/211[b]	148[f]
$PtC_{24}Pt$	227	128/145/169/193/213[b]	350[g]
$PtC_{28}Pt$	215	124/141/158/172/190[b]	350[g]

[a] Sealed; conventional melting point apparatus. [b] Exotherm. [c] Decomposition with liquefaction. [d] Endotherm; that of **PtC_6Si** is immediately followed by an exotherm. [e] Decomposition with melting. [f] Decomposition without melting. [g] There was no evident change in the appearance of the sample below this temperature.

workup. This compound was much more labile than **PtC_4H**, and darkened within a few minutes at room temperature. The hexatriynyl ^{13}C NMR signals exhibited coupling constant patterns (J(C,H), J(C,Pt), J(C,P)) that allowed unambiguous assignments (Table 3).

Another Hay cross coupling was conducted with **PtC_6H** and $HC{\equiv}CSiEt_3$. However, the target molecule **PtC_8Si** (yellow powder) was isolated in only 23% overall yield from **PtC_6Si**. The major product was the homocoupled species **$PtC_{12}Pt$** (38%), which is best prepared as described below. Analogous pentafluorophenyl platinum complexes also give increasing amounts of homocoupling with increasing sp carbon chain lengths.[13] The Brønsted acidities of terminal polyynes similarly increase with chain length.[23] Hence, there appears to be a correlation between the homocoupling/heterocoupling selectivities and the relative acidities of the reaction partners. We wondered whether higher homologues of $HC{\equiv}CSiEt_3$ might give better results. This would also enhance the efficiency of chain extension.

Thus, cross couplings of **PtC_xH** and trialkylsilylbutadiynes were investigated. However, reactions of **PtC_4H** and the readily available diyne $H(C{\equiv}C)_2SiMe_3$ were disappointing. Certain data suggested complications due to trimethylsilyl group cleavage. To enhance substitution stability, the triethylsilyl analogue $H(C{\equiv}C)_2SiEt_3$ was sought. Although this compound is known,[24] convenient large-scale syntheses are lacking. After several trials,[25] it was found that the sequential reaction of $H(C{\equiv}C)_2H$ with nBuLi (1.1 equiv) and $ClSiEt_3$ gave $H(C{\equiv}C)_2SiEt_3$ in 46% yield on an eight-gram scale. Some $Et_3Si(C{\equiv}C)_2SiEt_3$ also formed, but was easily separated by distillation.

As shown in Scheme 3 (top), **PtC_4H** and $H(C{\equiv}C)_2SiEt_3$ (20 equiv) were coupled under Hay conditions analogous to those used with $HC{\equiv}CSiEt_3$ in Scheme 2. Chromatography gave, in inverse order of elution, the target complex **PtC_8Si** (29%), the higher homologue **$PtC_{12}Si$** (30%; orange), and a small amount of the next highest homologue **$PtC_{16}Si$** (1%; deep red). Trace amounts of a material believed to be **$PtC_{20}Si$** were also isolated, but sufficed only for a UV/Vis spectrum. The simplest explanation for the formation of the higher homologues would involve the competitive desilylation of **PtC_xSi** under the reaction conditions. Indeed, small quantities of **PtC_8Si** could be detected in the above synthesis of **PtC_6Si** (Scheme 2). Also, UV/Vis data indicated the for-

Table 2. IR,[a] ^{31}P NMR,[b] and cyclic voltammetry[c] data.

	IR $\nu_{C\equiv C}$ [cm^{-1}]	$^{31}P\{^1H\}$ NMR δ [ppm] (^1J(P,Pt) [Hz])	$E_{p,a}$ [V]
PtC_4H	2138 (s)[d]	19.4 (2939)	–
PtC_6H	2154/2100/1992 (s/m/m)[e]	19.1 (2906)	–
PtC_4Si	2176/2126 (m/s)	22.1 (2966)	–
PtC_6Si	2146/2011 (s/s)	19.5 (2921)	–
PtC_8Si	2127/2081/2061/2003 (m/s/s/m)	19.2 (2902)	–
$PtC_{10}Si$	2162/2138/2057/1992 (w/w/s/s)	19.1 (2898)	–
$PtC_{12}Si$	2142/2114/2019/1984 (m/w/s/s)	19.0 (2892)	–
$PtC_{14}Si$	2171/2113/2007/1966 (w/m/m/s)	19.0 (2891)	–
$PtC_{16}Si$	2157/2130/2099/2074/2034/2045/1997/1941 (w/w/m/m/w/w/w/s)	19.0 (2889)	–
PtC_6Pt	2096 (w)	19.2 (2964)	0.855
PtC_8Pt	2135/1992 (m/w)	19.0 (2931)	0.971
$PtC_{10}Pt$	2144/2041 (m/m)	19.1 (2911)	1.091
$PtC_{12}Pt$	2131/2084/2011/1988 (m/s/w/m)	19.0 (2908)	1.204
$PtC_{16}Pt$	2162/2088/2042/1980 (w/m/s/s)	19.7 (2903)	1.264
$PtC_{20}Pt$	2144/2041/2011/1972/1922 (w/w/m/s/s)	19.0 (2889)	1.40[f]
$PtC_{24}Pt$	2135/2108/2061/1996/1953/1899 (w/w/w/m/s/m)	19.7 (2886)	[f]
$PtC_{28}Pt$	2148/2105/2084/2034/1987/1937/1887 (w/w/w/w/w/s/m)	19.7 (2885)	[f]

[a] Powder film. [b] In $CDCl_3$. [c] Scan rate 100 $mV s^{-1}$ under conditions described in the Experimental Section. [d] Additional band: 3293 (m, $\nu_{\equiv C\text{-}H}$). [e] additional band: 3312 (w, $\nu_{\equiv C\text{-}H}$). [f] Exact value difficult to estimate from voltammogram.

Table 3. ^{13}C NMR data (δ [ppm] in $CDCl_3$).

	Pt*C*≡ (^2J(C,P) [Hz])	Pt*C*≡*C*	C≡*C*Si	*C*≡CSi	Other
PtC$_4$H	110.6 (13.8)	95.3			72.9,[a,b] 58.1[b,c]
PtC$_6$H	117.4 (14.5)	96.0			71.5,[b,d] 66.0,[a,b] 64.7,[b,e] 54.8[b,c]
PtC$_4$Si	114.2 (–)	97.6	93.4	75.7	
PtC$_6$Si	117.5 (13.9)	95.8	91.8	79.1	66.6, 54.9
PtC$_8$Si	120.4 (13.6)	95.6	90.6	81.9	67.0, 64.8, 58.4, 55.1
PtC$_{10}$Si	122.4 (14.8)	95.4	89.8	84.1	67.1, 65.6, 63.5, 59.7, 58.7, 55.3
PtC$_{12}$Si	123.7 (13.9)	95.3	89.4	85.5	67.4, 66.0, 64.4, 62.8, 60.9, 60.1, 58.9, 55.3
PtC$_{14}$Si	124.6 (14.3)	95.2	89.1	86.5	67.6, 66.3, 64.7, 63.6, 62.3, 61.6, 61.2, 60.1, 58.8, 55.3
PtC$_{16}$Si	125.2 (14.5)	95.1	88.9	87.1	67.9, 66.6, 65.0, 63.9, 63.1, 62.1, 62.0,[f] 61.2, 60.1, 58.8, 55.4
PtC$_6$Pt	107.3 (15.3)	99.4	–	–	60.5
PtC$_8$Pt	112.9 (15.7)	97.6	–	–	63.8, 57.7
PtC$_{10}$Pt	117.3 (15.3)	96.5	–	–	64.7, 61.6, 56.8
PtC$_{12}$Pt	120.1 (14.5)	96.0	–	-	65.9, 63.2, 60.5, 56.1
PtC$_{16}$Pt	123.3 (14.5)	95.5	–	–	67.1, 65.3, 63.2, 61.3, 59.5, 55.7
PtC$_{20}$Pt	124.9 (14.5)	95.2	–	–	67.7, 66.4, 64.6, 63.2, 62.0, 60.6, 59.1, 55.6
PtC$_{24}$Pt	125.6 (–)	95.0	–	–	67.7, 66.6, 65.1, 64.0, 63.1, 62.2, 61.3, 60.1, 58.8, 55.3
PtC$_{28}$Pt	126.0 (–)	95.0	–	–	67.8, 66.9, 65.4, 64.5, 63.7, 63.1, 62.5, 61.8, 61.0, 60.0, 58.8, 55.3

[a] Pt*C*≡*CC*≡. [b] See Experimental Section for J(C,H) values that justify the assignment. [c] Pt*C*≡*CC*≡*C*. [d] Pt*C*≡*CC*≡*CC*≡. [e] Pt*C*≡*CC*≡*CC*≡*C*. [f] Two peaks overlapped.

Table 4. UV/Vis data.

	Absorption [nm] (ε [$M^{-1}cm^{-1}$])
PtC$_4$H[a]	317 (5840)
PtC$_6$Si[a]	321 (10600), 341 (6240), 365 (3040)
PtC$_8$Si[a]	255 (91000), 270 (80300), 301 (114000), 325 (69600), 384 (7120), 416 (4160)
PtC$_{10}$Si[a]	248 (92500), 260 (90900), 272 (76000), 288 (67800), 316 (107000), 342 (138000), 416 (2000) 450 (1120)
PtC$_{12}$Si[a]	257 (77100), 269 (79200), 283 (73600), 299 (78700), 316 (102000), 336 (97800), 368 (137000), 478 (800)
PtC$_{14}$Si[b]	263, 275, 289, 305, 321, 340, 362, 378, 384
PtC$_{16}$Si[b]	264, 277, 291, 306, 323, 341, 361, 385, 404
PtC$_{20}$Si[b]	278, 284, 307, 322, 338, 355, 375, 414, 418
PtC$_6$Pt[c]	329 (33600), 351 (25600), 376 (8800)
PtC$_8$Pt[c]	305 (99200), 337 (102000), 359 (17600), 387 (8800) 419 (5600)
PtC$_{10}$Pt[c]	281 (74400), 316 (110000), 327 (118000), 350 (213000), 391 (4640),[a] 424 (3680),[a] 463 (2480)[a]
PtC$_{12}$Pt[c]	323 (106000), 345 (201000), 371 (361000), 420 (2880),[a] 455 (1680),[a] 499 (880)[a]
PtC$_{16}$Pt[c]	293 (55200), 310 (50400), 335 (61600) 357 (103000), 383 (219000) 411 (365000)
PtC$_{20}$Pt[c]	280 (74400), 296 (71200), 312 (76800), 328 (80000), 347 (78400), 413 (262000), 444 (368000)
PtC$_{24}$Pt[c]	326 (115000), 341 (126000), 358 (127000), 379 (130000), 437 (307000), 472 (387000)
PtC$_{28}$Pt[c]	346 (170000), 363 (188000), 382 (190000), 457 (360000), 489 (402000)

[a] 1.25×10^{-5} M in CH_2Cl_2. [b] the amount of sample available did not allow the ε value to be determined. [c] 1.25×10^{-6} M in CH_2Cl_2.

mation of trace amounts of **PtC$_{16}$Pt**, **PtC$_{20}$Pt**, **PtC$_{24}$Pt**, and **PtC$_{28}$Pt** (see below).

As shown in Scheme 3 (bottom), **PtC$_6$H** was generated in situ from **PtC$_6$Si** and nBu$_4$N$^+$F$^-$, and treated with $ClSiMe_3$, which is believed to serve as a fluoride-ion scavenger. In previous work, this step was necessary for the success of subsequent Hay couplings.[13] Accordingly, the addition of $H(C{\equiv}C)_2SiEt_3$ (20 equiv) under the Hay conditions gave **PtC$_{10}$Si** (59%, orange) and **PtC$_{14}$Si** (7%, red). For some reason, this coupling is reproducibly more selective than that of **PtC$_4$H**. Trace quantities of a material believed to be **PtC$_{18}$Si** were also isolated, as evidenced by a UV/Vis spectrum.

Similar smaller scale exploratory sequences were conducted with **PtC$_8$Si** and **PtC$_{10}$Si**. The former gave **PtC$_{12}$Si** in 42% yield, and the latter **PtC$_{14}$Si** in 20% yield. Higher homologues presumably formed, but the scales were not sufficient for isolation. No attempts were made to detect the intermediates **PtC$_8$H** and **PtC$_{10}$H**; which are certain to be extremely labile. To our knowledge, **PtC$_{14}$Si** and **PtC$_{16}$Si** feature the longest sp carbon chains with a single transition-metal endgroup. Key spectroscopic data for **PtC$_x$Si** are summarized in Tables 1–3, including that of the previously reported complex **PtC$_4$Si**.[26]

Syntheses of diplatinum complexes: The homocoupling of **PtC$_x$H** under Hay conditions was investigated next. As shown in Scheme 4, the oxidation of **PtC$_4$H** at 40°C gave the yellow octatetraynediyl complex **PtC$_8$Pt** in 74% yield. The analogous reaction with isolated **PtC$_6$H** proceeded at room temperature, and afforded the bright orange dodecahexaynediyl complex **PtC$_{12}$Pt** in 83% yield. However, as noted above, **PtC$_6$H** is quite labile, and the feasibility of a one-pot synthesis from **PtC$_6$Si** was also tested. Accordingly, the sequential addition of nBu$_4$N$^+$F$^-$, $ClSiMe_3$, and the Hay coupling components gave **PtC$_{12}$Pt** in 88% yield. Thus,

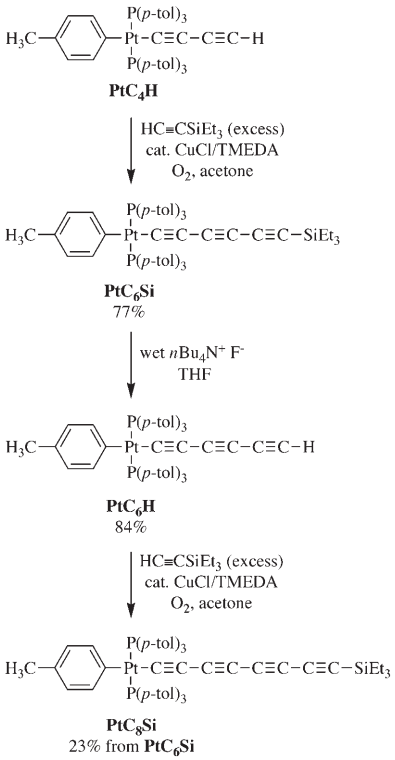

Scheme 2. Two-carbon sp chain extension reactions.

PtC_8Si was similarly converted to **PtC_8H** and subjected to the Hay conditions, but at 0 °C. Workup gave the red hexadecaoctaynediyl complex **$PtC_{16}Pt$** (70 %).

Given our past experiences with analogous pentafluorophenyl platinum complexes, we were doubtful that this methodology could be further extended.[13] Nonetheless, as shown in Scheme 4, **$PtC_{10}Si$** was analogously treated at −25 °C. Workup gave the red eicosadecaynediyl complex **$PtC_{20}Pt$** in 72 % yield, only the second such species to be isolated in significant quantity.[11a] However, when similar sequences were conducted with **$PtC_{12}Si$** at −25 °C or −45 °C, no tractable products could be isolated. Under these conditions, the rate of decomposition of the intermediate **$PtC_{12}H$** is presumably too fast. Importantly, a $ClSiMe_3$ treatment step must be survived before any oxidizing agent is encountered. However, note the steadily decreasing temperature requirement for the homocoupling of **PtC_xH** as the chain is lengthened.

Thus, a modified procedure was attempted. Qualitatively, the rates of desilylation of **PtC_xSi** appeared to increase with chain length, in accord with the leaving-group abilities expected from the Brønsted acidity trends given above.[23] Also, desilylation somehow occurs under the conditions of Scheme 3 (top), in which fluoride ion is absent. We therefore wondered whether **$PtC_{12}Si$** might undergo protodesilylation under the Hay homocoupling conditions.[27] Since **$PtC_{12}H$** would then be generated in the presence of an oxidizing agent, there would be a better chance that homocoupling could compete. As shown in Scheme 4, **$PtC_{12}Si$** was

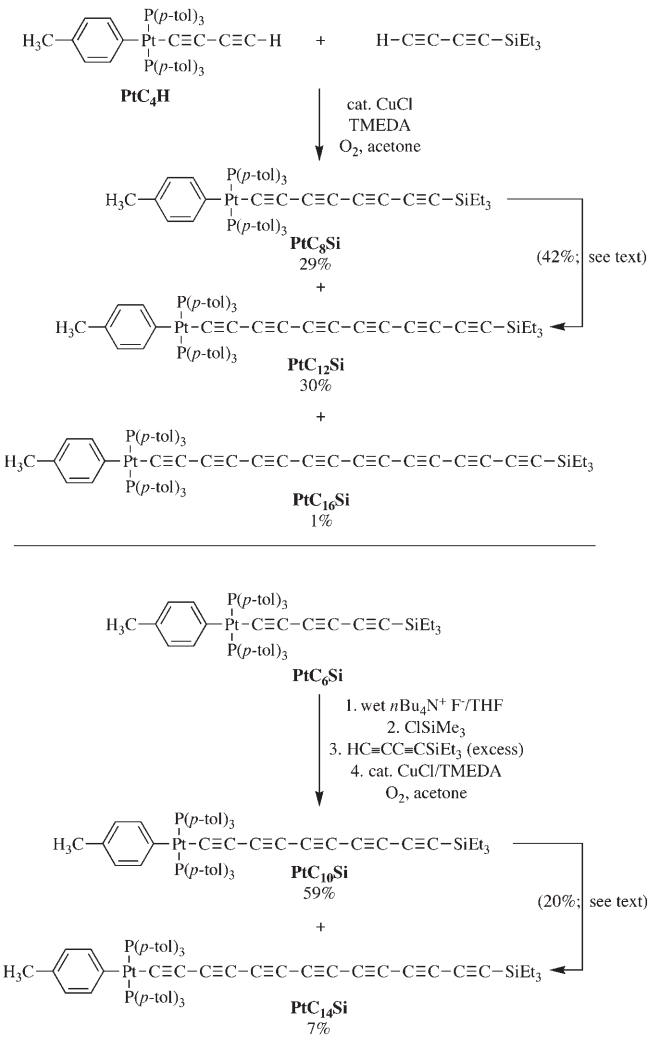

Scheme 3. Four-carbon sp chain extension reactions.

treated under such conditions at 10 °C. Indeed, chromatography gave the deep red tetracosadodecaynediyl complex **$PtC_{24}Pt$** in 36 % yield, along with 38 % of recovered **$PtC_{12}Si$**. A similar reaction of **$PtC_{14}Si$** at 0 °C gave the deep red octacosatetradecaynediyl complex **$PtC_{28}Pt$** in 51 % yield, shattering existing length records for C_x complexes.

As a final synthetic challenge, analogous complexes with odd numbers of triple bonds were sought. These cannot be accessed by homocouplings. Thus, the cross coupling sequence in Scheme 5 (top, A) was attempted. First, **PtC_6H** was generated in situ from **PtC_6Si** as described above. Then **PtCl**, together with $HNEt_2$ and a catalytic amount of CuI, was added. This models the coupling conditions for **PtCl** and $H(C{\equiv}C)_2H$ in Scheme 1. Workup gave the yellow hexatriynediyl complex **PtC_6Pt** in 56 % yield. An analogous sequence was conducted with **$PtC_{10}Si$** at 0 °C. As shown in Scheme 5 (bottom), workup gave the orange decapentaynediyl complex **$PtC_{10}Pt$** in 84 % yield. However, a similar attempt to convert **$PtC_{14}Si$** to the tetradecaheptaynediyl complex **$PtC_{14}Pt$** was unsuccessful. This constitutes further evi-

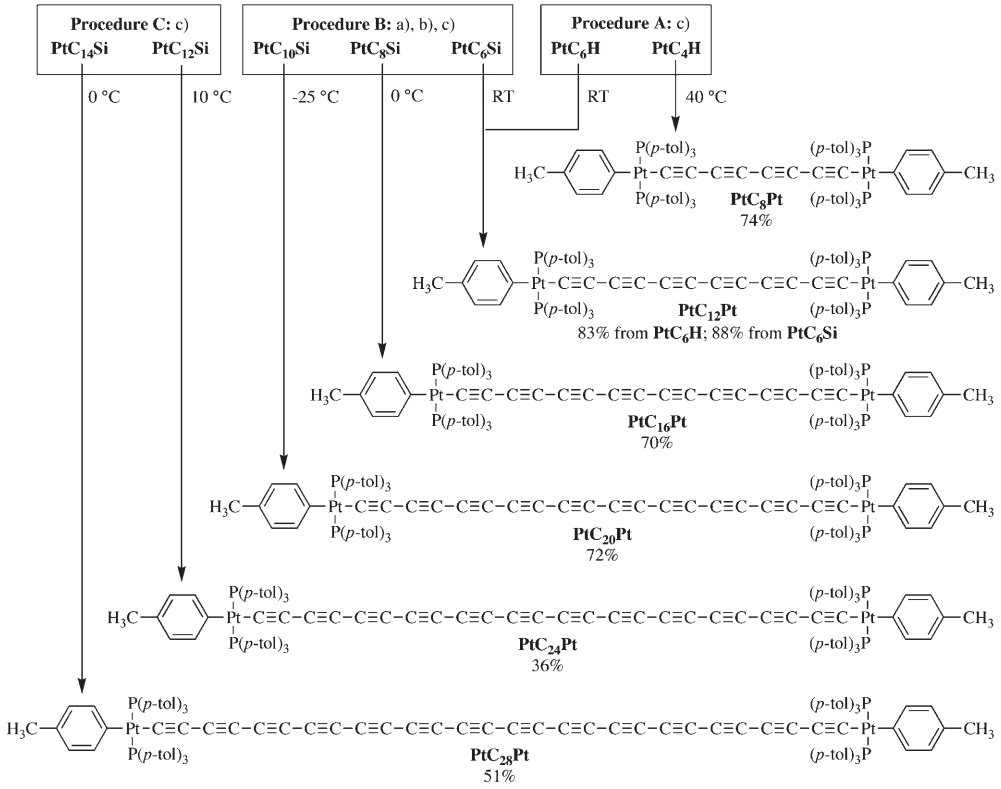

Scheme 4. Syntheses of diplatinum polyynediyl complexes with even numbers of C≡C bonds: a) wet nBu$_4$N$^+$F$^-$/Acetone; b) ClSi(CH$_3$)$_3$; c) cat. CuCl/TMEDA, O$_2$, Acetone.

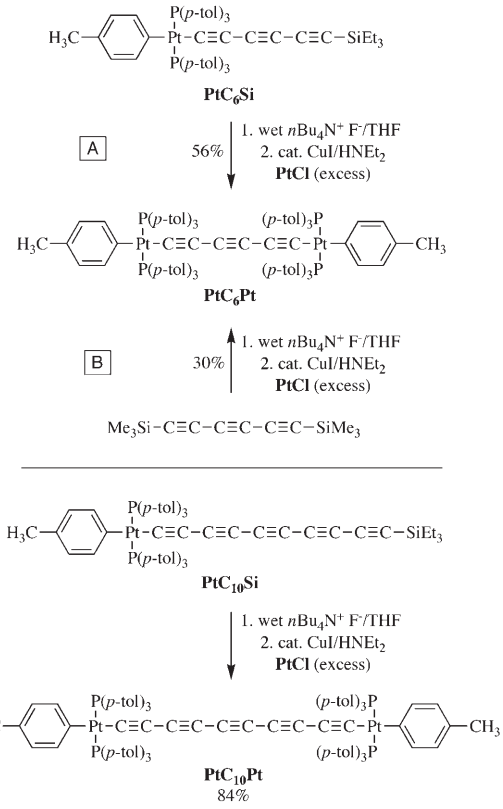

Scheme 5. Syntheses of diplatinum polyynediyl complexes with odd numbers of C≡C bonds.

dence for the rapid decomposition of **PtC$_x$H** ($x \geq 12$) generated from nBu$_4$N$^+$F$^-$ in wet THF.

An alternative strategy would entail the bis(functionalization) of organic polyynes. As shown in Scheme 5 (top, B), the readily available triyne Me$_3$Si(C≡C)$_3$SiMe$_3$[28] was treated with wet nBu$_4$N$^+$F$^-$ (2.0 equiv) at −78 °C to generate H(C≡C)$_3$H. This was added to **PtCl** (2.0 equiv), HNEt$_2$, and a catalytic amount of CuI at −45 °C. Workup gave **PtC$_6$Pt** in 30% yield, slightly less than the overall yield from **PtCl** in synthesis A (35%). In the early stages of this project, a related sequence was attempted with the octatetrayne Me$_3$Si(C≡C)$_4$SiMe$_3$.[29] Less than one equivalent of **PtCl** was used, in hopes of selectively generating **PtC$_8$H**. Then the Hay conditions were applied. Small quantities of the target complex **PtC$_{16}$Pt** were isolated. However, numerous other products formed, including **PtC$_8$Pt** and the trimethylsilyl analogue of **PtC$_8$Si**. The latter presumably arises from incomplete desilylation.[30]

The complexes **PtC$_6$Pt**, **PtC$_8$Pt**, **PtC$_{10}$Pt**, **PtC$_{12}$Pt**, **PtC$_{16}$Pt**, **PtC$_{20}$Pt**, **PtC$_{24}$Pt**, and **PtC$_{28}$Pt** were isolated as air-stable, analytically pure powders. In the cases of **PtC$_{20}$Pt**, **PtC$_{24}$Pt**, and **PtC$_{28}$Pt**, there was no significant decomposition over a period of several days, although slow decomposition occurred in solution. Lower homologues were stable for months. As noted above, the colors progressively deepened from yellow (**PtC$_6$Pt**) to orange (**PtC$_{10}$Pt**) to red (**PtC$_{16}$Pt**) to deep red (**PtC$_{24}$Pt**), consistent with the UV/Vis data given in

Table 4. Spectra for the entire series are illustrated in Figure 1 and further analyzed below.

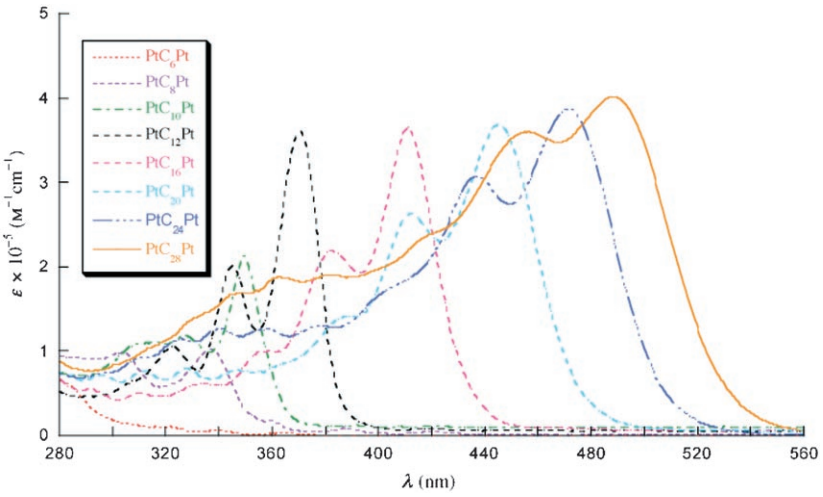

Figure 1. UV/Vis spectra of **PtC$_x$Pt** (1.25×10^{-6} M in CH_2Cl_2).

DSC and TGA measurements indicated excellent thermal stabilities, as summarized in Table 1.[31] The former revealed exothermic decompositions that could be grouped as follows. From **PtC$_{10}$Pt** through **PtC$_{16}$Pt**, the T_i and T_e values[31] were about 200 °C. However, those for **PtC$_{20}$Pt**, **PtC$_{24}$Pt**, and **PtC$_{28}$Pt** showed steady decreases, first to about 150 °C and then 140 °C (T_e). The shorter-chain complexes **PtC$_6$Pt** and **PtC$_8$Pt** exhibited exotherms at similar temperatures. Nonetheless, in no case did any mass loss occur below 200 °C. Visually, no phase transitions or signs of decomposition were apparent when **PtC$_{24}$Pt** and **PtC$_{28}$Pt** were heated to 350 °C in capillaries. These data, and the spectroscopic properties summarized in Tables 2–4, are further analyzed in the Discussion section.

Crystallography and cyclic voltammetry: In the course of characterizing **PtC$_x$Si** and **PtC$_x$Pt**, extensive attempts were made to obtain crystals. The crystal structures of seven complexes or solvates thereof could be determined as summarized in Table 5 and the Experimental Section. The molecular structures are illustrated in Figures 2 and 3, and analyzed below. Key bond lengths and angles, and other structural parameters, are listed in Tables 6 and 7, together with those of the previously characterized **PtC$_4$Si** complex.[26] One complex, designated as **Pt′C$_8$Pt′**, features PPh_3 instead of P(*p*-tol)$_3$ ligands, and was prepared by an analogous sequence described earlier.[15a]

All of the diplatinum complexes exhibited an inversion center. One consequence is that the coordination planes of the platinum endgroups define angles of 0° (e.g., (C_{ipso}-PPt_1P-C_α) vs. (C_{ipso}-PPt_2P-C_α)). However, as established by a recent computational study,[32] there is no electronic basis for this orientation. It apparently reflects a deep-seated packing preference.

The packing diagrams were also analyzed. A representative case is shown in Figure 4, and others are provided in the Supporting Information. All of the complexes except one crystallized in motifs with a single set of parallel chains. The exception, **PtC$_8$Si**, exhibited two non-parallel sets of parallel chains. Both patterns have extensive precedent in conjugated polyynes.[4] The parallel chains nearest to each other were identified, and the shortest C_{sp}–C_{sp} distance calculated (Tables 6 and 7). There is a tendency for the endgroup of one molecule to nest along the carbon chain of its neighbor, as any dumbbell-shaped object would be expected to pack. Thus, the endgroups are "offset"[4] in the longer chain complexes **PtC$_8$Si**, **PtC$_{10}$Si**, **Pt′C$_8$Pt′**, **PtC$_{10}$Pt**, and **PtC$_{12}$Pt** by 0.76, 0.13, 0.38, 0.88, and 0.45 of the platinum–silicon or platinum–platinum distance. The nearest chains in **PtC$_8$Si** and **PtC$_{10}$Si** adopt "head-to-tail" arrangements.

Complexes with chains longer than C_{12} are conspicuously absent among the structures in Figures 2 and 3. The pentafluorophenyl complex analogous to **PtC$_{16}$Pt** crystallizes,[13] but only with a large amount of solvent (ten molecules of benzene). Perhaps the bulky endgroups in **PtC$_x$Pt** enforce spatial voids at long chain lengths that that are difficult to fill except with large quantities of easily volatilized or disordered solvent. The use of larger solvents or guest molecules might possibly help in future work. Nonetheless, from the data for **PtC$_{12}$Pt** in Table 7, the platinum–platinum distance in **PtC$_{28}$Pt** can be estimated as 38.8 Å.

Finally, oxidation reactions of **PtC$_x$Pt** were studied by cyclic voltammetry in CH_2Cl_2. As summarized in Table 2, they appeared to become thermodynamically more difficult at longer chain lengths, as evidenced by increasingly positive $E_{p,a}$ values. The electronic basis for this trend, which is counterintuitive from the standpoint of organic polyynes, has been detailed in a computational study.[32] As expected, all complexes were more easily oxidized than the pentafluorophenyl analogues.[13,33] However, the oxidation reactions were less reversible than those of the pentafluorophenyl analogues. As illustrated in the Supporting Information, additional peaks suggestive of electrode/chemical/electrode (ECE) processes were often observed, and in most cases there was no appreciable cathodic current. Hence, the $E_{p,a}$ values can only be taken as rough guides to the relative oxidation potentials.

Table 5. Summary of crystallographic data.

	PtC$_6$Si	**PtC$_8$Si**·(CH_2Cl_2)	**PtC$_{10}$Si**	**PtC$_6$Pt**·(benzene)$_2$	**Pt′C$_8$Pt′**·(acetone)$_4$·(1,2-difluorobenzene)$_{0.5}$	**PtC$_{10}$Pt**	**PtC$_{12}$Pt**·(benzene)$_2$
formula	$C_{61}H_{64}P_2PtSi$	$C_{64}H_{66}P_2Cl_2PtSi$	$C_{65}H_{64}P_2PtSi$	$C_{116}H_{110}P_4Pt_2$	$C_{109}H_{100}FO_4P_4Pt_2$	$C_{108}H_{98}P_4Pt_2$	$C_{122}H_{110}P_4Pt_2$
M_r	1082.24	1191.19	1130.28	2018.10	2006.95	1909.92	2090.16
diffractometer	Nonius KappaCCD	Nonius KappaCCD	Nonius KappaCCD	Nonius KappaCCD	Bruker AXS	Nonius KappaCCD	Bruker AXS
T [K]	173(2)	173(2)	173(2)	173(2)	148(2)	173(2)	200(0.1)
λ [Å]	0.71073	0.71073	0.71073	0.71073	0.71073	0.71073	0.71073
crystal system	triclinic	monoclinic	triclinic	triclinic	triclinic	triclinic	triclinic
space group	$P\bar{1}$	$P2_1/n$	$P\bar{1}$	$P\bar{1}$	$P\bar{1}$	$P\bar{1}$	$P\bar{1}$
a [Å]	13.0890(2)	10.7470(2)	11.9890(6)	11.22840(10)	10.2030(6)	12.0546(3)	11.1276(3)
b [Å]	13.1770(2)	23.2570(5)	14.9290(5)	13.2052(2)	11.5755(6)	13.8864(2)	14.1781(2)
c [Å]	15.6040(3)	23.4960(4)	16.6850(9)	18.5067(3)	21.4583(13)	15.7611(3)	17.2390(3)
α [°]	91.1380(10)	90	82.029(3)	69.7490(10)	90.468(3)	112.923(1)	81.5013(11)
β [°]	91.9070(10)	95.1490(12)	77.913(2)	86.8410(10)	102.495(4)	100.302(1)	73.1268(8)
γ [°]	90.0710(10)	90	71.852(3)	70.6660(10)	114.054(3)	100.767(1)	79.3074(11)
V [Å^3]	2689.25(8)	5848.96(19)	2766.2(2)	2423.75(6)	2246.2(2)	2293.05(8)	2544.70(9)
Z	2	4	2	1	1	1	1
ρ_{calcd} [Mg m^{-3}]	1.337	1.353	1.357	1.385	1.484	1.383	1.364
μ [mm^{-1}]	2.727	2.603	2.655	2.997	3.238	3.164	2.857
$F(000)$	1104	2424	1152	1022	1011	962	1058
crystal size [mm^3]	0.20×0.2×0.15	0.20×0.15×0.10	0.20×0.10×0.05	0.35×0.30×0.15	0.32×0.21×0.05	0.40×0.30×0.20	0.23×0.14×0.08
θ range [°]	1.31–27.51	1.23–27.53	1.98–25.11	1.18–27.45	1.94–28.32	1.66–27.46	3.54–33.64
index range	$-16\le h\le 17$ $-17\le k\le 17$ $-20\le l\le 17$	$-13\le h\le 13$ $-28\le k\le 30$ $-30\le l\le 30$	$-14\le h\le 14$ $-16\le k\le 17$ $-19\le l\le 19$	$-14\le h\le 14$ $-17\le k\le 17$ $-24\le l\le 22$	$-6\le h\le 13$ $-14\le k\le 13$ $-28\le l\le 28$	$-15\le h\le 15$ $-17\le k\le 18$ $-19\le l\le 20$	$0\le h\le 17$ $-19\le k\le 19$ $-25\le l\le 26$
reflns collected	23316	24263	18604	20675	14919	19838	12868
independent reflns	12320	13343	9762	10998	10277	10461	12868
reflns [$I>2\sigma(I)$]	11022	9162	7406	9408	8385	9093	12868
max/min transmission	0.6851/0.6115	0.7808/0.6241	0.8787/0.6188	0.6620/0.4202	0.9281/0.6629	0.5703/0.3643	0.5594/0.8036
data/restraints/parameters	12320/1/596	13343/0/641	9762/0/622	10998/0/550	10277/17/547	10461/0/514	12868/0/578
GOF on F^2	1.007	1.018	0.992	1.047	0.937	1.025	1.049
final R indices	$R1=0.0265$	$R1=0.0413$	$R1=0.0399$	$R1=0.0320$	$R1=0.0396$	$R1=0.0301$	$R1=0.0375$
[$I>2\sigma(I)$]	$wR2=0.0639$	$wR2=0.0935$	$wR2=0.0841$	$wR2=0.0731$	$wR2=0.0782$	$wR2=0.0745$	$wR2=0.0718$
R indices	$R1=0.0324$	$R1=0.0784$	$R1=0.0654$	$R1=0.0433$	$R1=0.0529$	$R1=0.0389$	$R1=0.0375$
(all data)	$wR2=0.0679$	$wR2=0.1124$	$wR2=0.0922$	$wR2=0.0791$	$wR2=0.0815$	$wR2=0.0781$	$wR2=0.0718$
largest diff. peak/hole [e Å^3]	0.473/−1.048	1.619/−1.191	0.945/−0.859	1.860/−1.640	1.727/−1.482	1.157/−2.890	2.027/−0.799

Discussion

Synthesis: Strategic considerations: The cross couplings of **PtC$_x$H** and HC≡CSiEt$_3$ in Scheme 2 parallel those reported earlier for analogous pentafluorophenyl platinum complexes.[13] An advantage adding two sp carbons stepwise is that in theory, all complexes **PtC$_x$Pt** with even numbers of C≡C bonds can be accessed. However, despite the large excesses of HC≡CSiEt$_3$ employed, progressively more homocoupling of **PtC$_x$H** occurs with increasing chain length. Useful quantities of decapentaynyl complexes (e.g., **PtC$_{10}$Si**) cannot be prepared in either series. Fortunately, as illustrated in Scheme 3, doubling the chain length of the silylated alkyne renders cross coupling more competitive. Given the empirical correlation with the relative acidities of the coupling partners noted above, the triyne H(C≡C)$_3$SiEt$_3$ would be even more effective. However, this labile compound has only been generated in solution, and the synthetic sequence is tedious.[24a]

Unfortunately, reactions of **PtC$_x$H** and H(C≡C)$_2$SiEt$_3$ are complicated by multiple cross couplings. We provisionally attribute this to subsequent in situ desilylation of the initial product to give **PtC$_{x+4}$H**. Reactions with excess diyne would then yield **PtC$_{x+8}$Si**. Note that multiple couplings occur in reactions in which fluoride ion is both absent (Scheme 3, top) and present (Scheme 3, bottom). In all cases chloride ions are available from CuCl, and sometimes from ClSiMe$_3$. Experiments to probe this mechanistic model and related points, for example, the effect of chain length upon cross-coupling rates, remain in progress.

Other in situ desilylations constitute key steps in the syntheses of the "record setting" complexes **PtC$_{24}$Pt** and **PtC$_{28}$Pt**. As shown in Scheme 4, **PtC$_{12}$Si** and **PtC$_{14}$Si** are apparently converted to **PtC$_{12}$H** and **PtC$_{14}$H** under the Hay conditions. Perhaps chloride ion or adventitious water from the acetone solvent play critical roles. Importantly, homocoupling now becomes much faster than decomposition. As reflected by the appreciable amount of starting **PtC$_{12}$Si** recovered in the synthesis of **PtC$_{24}$Pt**, this route appears limited to reactants **PtC$_x$Si** with very long chain lengths, such that the PtC$_x$ moiety becomes a sufficiently good leaving group.

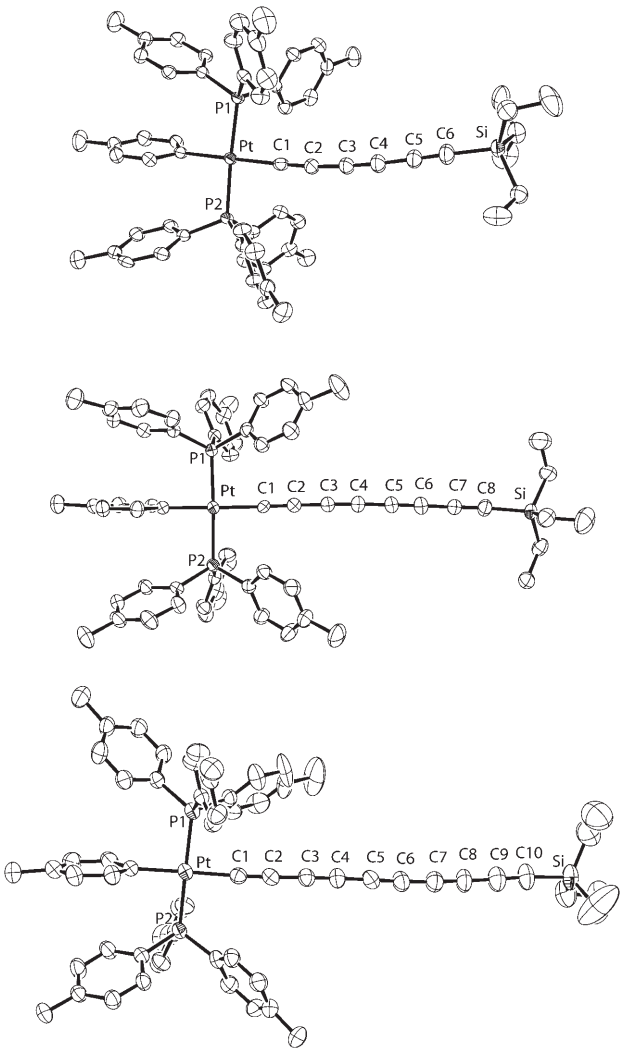

Figure 2. Structures of **PtC_6Si**, **PtC_8Si**·(CH_2Cl_2), and **$PtC_{10}Si$** with solvent molecules omitted.

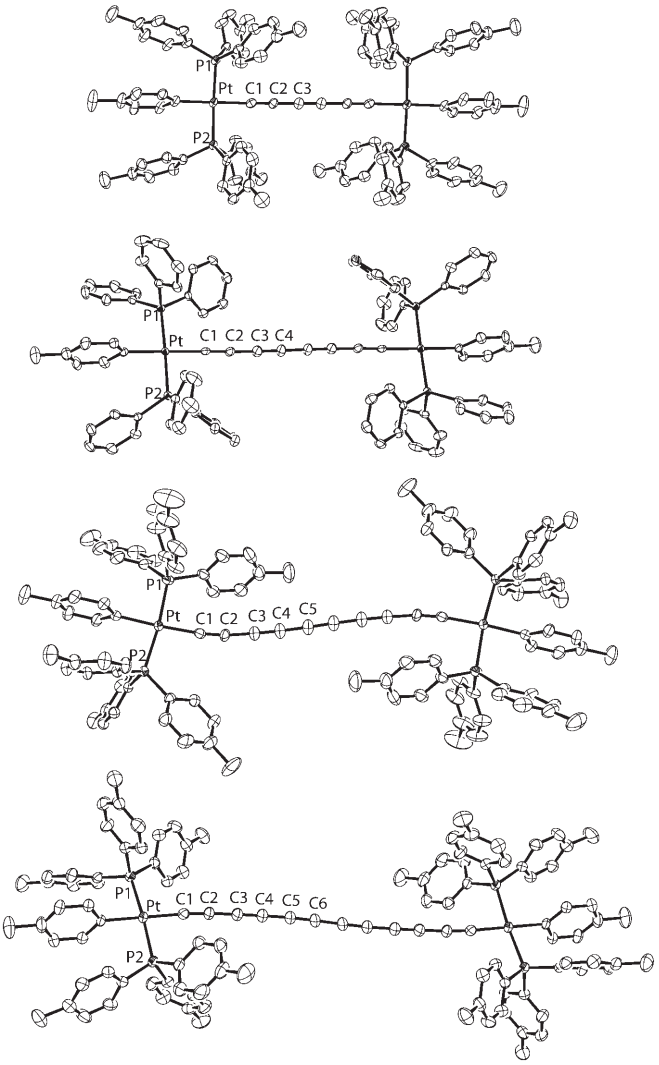

Figure 3. Structures of **PtC_6Pt**·(benzene)$_2$, **$Pt'C_8Pt'$**·(acetone)$_4$·(1,2-difluorobenzene)$_{1.5}$, **$PtC_{10}Pt$**, and **$PtC_{12}Pt$**·(benzene)$_2$ with solvent molecules omitted.

In terms of synthesis strategy, these data show that the limiting problem is not the stability of the target polyynediyl complexes **PtC_xPt**, but rather the precursors **$PtC_{x/2}H$**. Towards this end, the development of homocoupling methodologies that can make direct use of $[(L)_mM(C{\equiv}C)_nSiR_3]$ species, or possibly tin analogues, should greatly aid the further progress of this field. There are other promising new synthetic routes to long polyynes being developed, the most advanced of which involve the Fritsch–Buttenberg–Wiechell rearrangement.[34] However, in efforts to date with hexadecaoctaynes, yields are still quite modest.

Several possible extensions of our methodology merit emphasis. First, reactions of the types in Scheme 3 might be conducted with still larger excesses of $H(C{\equiv}C)_2SiEt_3$, and for extended periods, such that oligomerization to **PtC_xSi** with $x>20$ occurs. Given the ready chromatographic separation of the complexes with $x>20$ described above, the chances are good that mixtures of much higher oligomers can also be purified, as long as they are sufficiently stabile. Second, these could be evaluated as precursors to complexes **PtC_xPt** with substantially longer chains than in Scheme 4. Third, might more controlled cross couplings be realized with trialkylsilylbutadiynes that are less readily desilylated, such as the TIPS' derivative $H(C{\equiv}C)_2Si(i\mathrm{Pr})_3$?[35]

Thermal and oxidative stabilities: Polyynes normally possess highly positive heats of formation,[36] and may be regarded as energy-rich materials that are intrinsically thermodynamically unstable. Transition-metal endgroups are electropositive and usually quite bulky. Hence, they are believed to provide both steric and electronic stabilization. Importantly, we have never encountered any explosions when handling complexes of the formula $[(L)_mM(C{\equiv}C)_nM(L)_m]$ or $[(L)_mM(C{\equiv}C)_nX]$. In contrast, a variety of organic and halogenated polyynes are known to detonate.

As summarized in Table 1, **$PtC_{10}Pt$**, **$PtC_{12}Pt$**, and **$PtC_{16}Pt$** exhibit an exotherm and mass loss at approximately the

Table 6. Key interatomic distances [Å] and bond angles [°] for **PtC$_x$Si**.

	PtC$_4$Si	**PtC$_6$Si**	**PtC$_8$Si**	**PtC$_{10}$Si**
Pt−C1	2.039(15)	2.014(3)	2.008(5)	1.992(6)
C1≡C2	1.196(18)	1.210(4)	1.217(7)	1.219(7)
C2−C3	1.37(2)	1.364(4)	1.344(8)	1.375(8)
C3≡C4	1.196(18)	1.213(4)	1.221(8)	1.200(8)
C4−C5 or C4−Si	1.832(16)	1.364(4)	1.355(8)	1.344(8)
C5≡C6	–	1.208(4)	1.203(8)	1.220(8)
C6−C7 or C6−Si	–	1.833(3)	1.358(8)	1.355(9)
C7≡C8	–	–	1.225(8)	1.209(8)
C8−C9 or C8−Si	–	–	1.833(6)	1.363(9)
C9≡C10	–	–	–	1.213(9)
C10−Si	–	–	–	1.842(7)
Pt···Si	7.602	10.151	12.732	15.266
sum of all bond lengths from Pt to Si	7.633	10.206	12.764	15.332
Pt−P1	2.302(3)	2.3040(6)	2.3008(12)	2.3024(13)
Pt−P2	2.311(3)	2.2933(6)	2.3056(12)	2.3026(13)
Pt−C$_{ipso}$	2.080(13)	2.067(3)	2.055(5)	2.052(6)
Pt-C1-C2	175.0(11)	177.8(2)	175.8(5)	176.4(5)
C1-C2-C3	178.1(14)	174.9(3)	178.4(6)	174.1(6)
C2-C3-C4	176.8(15)	176.8(3)	178.5(7)	177.8(6)
C3-C4-C5 or C3-C4-Si	174.0(13)	176.6(3)	177.8(7)	177.4(7)
C4-C5-C6	–	178.7(4)	179.0(8)	178.7(7)
C5-C6-C7 or C5-C6-Si	–	174.8(3)	177.1(7)	177.2(7)
C6-C7-C8	–	–	177.2(7)	177.4(7)
C7-C8-C9 or C7-C8-Si	–	–	173.3(5)	179.3(8)
C8-C9-C10	–	–	–	177.7(8)
C9-C10-Si	–	–	–	175.3(7)
average, Pt-C1-C2, C$_{sp}$-C$_{sp}$-C$_{sp}$, C$_{sp}$-C$_{sp}$-Si	176.0	176.6	177.1	177.1
shortest C$_{sp}$−C$_{sp}$ distance between parallel chains	7.133	5.687	5.025	7.036

Table 7. Key interatomic distances [Å] and bond angles [°] for **PtC$_x$Pt**.

	PtC$_6$Pt	**Pt′C$_8$Pt′**	**PtC$_{10}$Pt**	**PtC$_{12}$Pt**
Pt−C1	2.030(3)	2.011(4)	1.990(3)	1.990(3)
C1≡C2	1.193(5)	1.218(6)	1.190(5)	1.233(4)
C2−C3	1.388(5)	1.368(6)	1.404(4)	1.358(4)
C3≡C3′ or C3≡C4	1.211(7)	1.223(6)	1.215(5)	1.210(5)
C4−C5 or C4−C4′	–	1.367(9)	1.342(5)	1.356(5)
C5≡C5′ or C5≡C6	–	–	1.228(7)	1.211(5)
C6−C6′	–	–	–	1.344(7)
Pt1···Pt2	10.4058	12.998(1)	15.3730(3)	17.9564(4)
sum of all bond lengths from Pt1 to Pt2	10.433	13.007	15.510	18.060
Pt−P1	2.2993(8)	2.3002(11)	2.3012(8)	2.3055(8)
Pt−P2	2.2946(9)	2.3073(11)	2.3102(9)	2.3164(8)
Pt−C$_{ipso}$	2.056(3)	2.064(4)	2.078(3)	2.060(3)
Pt-C1-C2	174.0(3)	178.0(4)	173.2(3)	174.0(3)
C1-C2-C3	176.8(4)	176.5(5)	171.1(4)	174.5(4)
C2-C3-C3′ or C2-C3-C4	179.3(6)	177.8(5)	177.1(4)	178.6(4)
C3-C4-C4′ or C3-C4-C5	–	179.5(9)	176.4(4)	178.3(4)
C4-C5-C6	–	–	178.5(6)	177.5(4)
C5-C6-C6′	–	–	–	178.9(6)
average, Pt-C1-C2 and C$_{sp}$-C$_{sp}$-C$_{sp}$	176.7	178.0	175.3	177.0
shortest C$_{sp}$−C$_{sp}$ distance between parallel chains	10.137	8.916	8.489	7.884

same temperatures ($\geq$200 °C), suggesting a coupled process. However, with **PtC$_6$Pt** and **PtC$_8$Pt**, the first exotherm occurs at a much lower temperature than mass loss (140–150 °C (T_e) vs. 221 °C).[31] One possibility would be some type of sp-chain/sp-chain coupling or polymerization, as well documented for many 1,3-butadiynes in the solid state.[4,37] The longer chain complexes **PtC$_{20}$Pt**, **PtC$_{24}$Pt**, and **PtC$_{28}$Pt** also exhibit exotherms at lower temperatures (150–140 °C). In no cases are endotherms, indicative of reversible phase transitions such as melting, observed. In any event, the appreciable thermal stabilities of **PtC$_{24}$Pt** and **PtC$_{28}$Pt** support the supposition that higher homologues are viable synthetic targets. Note that the longer chain monoplatinum complexes **PtC$_{10}$Si**, **PtC$_{12}$Si**, and **PtC$_{14}$Si** also exhibit exotherms at lower temperatures (ca. 170–140 °C) than their lower homologues.

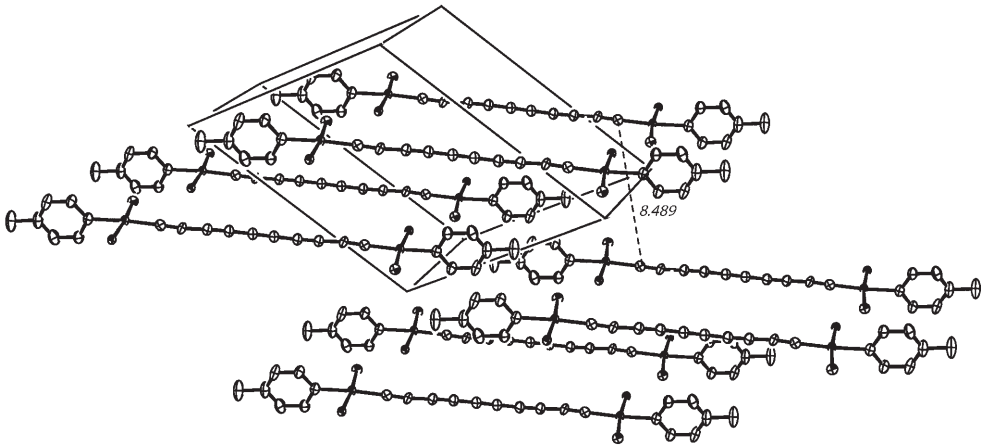

Figure 4. Representative packing diagram: **PtC$_{10}$Pt** with P*p*-tol$_3$ rings omitted and closest chain/chain contact illustrated.

Literature data for organic polyynes often indicate lower stability thresholds. For example, *tert*-butyl capped species $Me_3C(C{\equiv}C)_nCMe_3$ with $n=4$–8, 10, and 12 have been isolated, but that with $n=12$ decomposed within 8 min at room temperature to an insoluble black material.[38] In the triethylsilyl series $Et_3Si(C{\equiv}C)_nSiEt_3$, compounds with $n=6$ and 8 were isolable, but decomposed at room temperature or below; higher homologues ($n=10$, 12, 16) were only generated in solution.[24a] Tykwinski has recently shown that analogues with bulkier tri(isopropyl)silyl endgroups ($n=8$, 10) are stable to $>105\,^{\circ}C$.[34] Also, Hirsch has described two polyyne series with 3,5-disubstituted aryl endgroups, the highest members of which ($n=8$–10) were stable solids at room temperature.[39] Perhaps it will eventually be possible to isolate stable molecules in some of these newer series with chains longer than C_{20}.

As noted above, the title complexes show no significant decomposition as solids in air over periods ranging from days to months. However, the exceedingly poor reversibilities of the electrochemical oxidations are surprising, given the significant reversibilities with pentafluorophenyl analogues with C_4–C_8 chains.[13] We presume, by analogy to literature precedent,[40] that the initial step in both series involves a Pt^{II}/Pt^{III} couple, giving a mixed valence complex. Perhaps the fluorine substituents in some way hinder a subsequent chemical reaction that involves the aryl substituent.

IR and NMR spectra: Both **PtC$_x$Si** and **PtC$_x$Pt** exhibit a constant set of IR absorptions arising from the endgroups. The distinctive $\nu_{C{\equiv}C}$ bands are summarized in Table 2, and show several trends. First, most of the monoplatinum complexes exhibit more bands than diplatinum complexes of the same chain length, consistent with their lower symmetry. Second, the number of bands increases with chain length, in agreement with computational studies of organic polyynes.[41] For the diplatinum complexes, this corresponds to approximately one band per two C≡C units. The extinction coefficient of the most intense band, as normalized to the endgroup absorptions, also increases with chain length. Finally, the frequencies tend to be slightly lower than those of pentafluorophenyl analogues.[13]

With regard to the NMR data, the ^1J(P,Pt) values (Table 2) show a striking chain-length effect, monotonically decreasing for higher values of x or the number of C≡C units n. The value of any measurable quantity for a series of conjugated polyynes can be plotted versus $1/n$. An extrapolation to the y intercept ($1/n=0$) then gives the hypothetical value for the infinite-chain species. In the cases of **PtC$_x$Si** and **PtC$_x$Pt**, such plots are not very linear (see Supporting Information). Nonetheless, values of 2880 ± 4 Hz can be confidently predicted for both **PtC$_\infty$Si** and **PtC$_\infty$Pt**.

With aryl bis(phosphine) platinum complexes of the formula *trans*-$[Pt(p\text{-}ZC_6H_4)(PEt_3)_2X]$ (X = Br, H), the ^1J(P,Pt) values decrease as the group Z becomes more electron-withdrawing.[42] Thus, the trends in Table 2 provide further evidence for the increasing electronegativity of longer $(C{\equiv}C)_n$ chains, as invoked above to rationalize relative desilylation rates and other phenomena. Complementary data are provided by the IR ν_{NO} values of analogues with rhenium nitrosyl endgroups, which progressively increase with chain length.[11a] Enhanced electronegativity also accounts for the about 10% lower ^1J(P,Pt) values of the analogous pentafluorophenyl complexes.[13] However, the ^{31}P NMR chemical shifts (Table 2) do not show a clear trend with chain length, likely due to the magnitude of the measurement error.

The ^{13}C NMR data (Table 3) show a number of conspicuous trends. First, the Pt*C*≡ signals of both **PtC$_x$Si** and **PtC$_x$Pt** shift monotonically downfield with increasing chain length ($\Delta\delta=11.0$ and 18.3 ppm). Plots versus $1/n$ are quite linear ($R>0.997$; Supporting Information), and give a limiting chemical shift of $\delta=131\pm2$ ppm for both **PtC$_\infty$Si** and **PtC$_\infty$Pt**. The coupling constants ^2J(C,P) can also be examined for trends. However, the Pt*C*≡ signals are further coupled to ^{195}Pt (abundance 33.8%). This decreases the intensity of the main peak and renders the splitting more difficult to accurately determine, and sometimes impossible to observe.

The Pt*C*≡*C* signals of **PtC$_x$Si** and **PtC$_x$Pt** fall into a narrower chemical shift range ($\Delta\delta=2.5$ and 4.4 ppm). They move downfield with increasing chain length, reaching a limit of $\delta=94.5\pm0.2$ ppm for both series of compounds. In the case of **PtC$_x$Si**, the ≡*C*Si signal undergoes a downfield shift ($\Delta\delta=11.4$ ppm), while the downfield *C*≡CSi signal undergoes a upfield shift ($\Delta\delta=4.5$ ppm). When **PtC$_{16}$Si** is reached, the signals that were once widely separated in **PtC$_4$Si** are nearly degenerate ($\Delta\delta=12.7$ vs. 1.8 ppm). For **PtC$_\infty$Si**, plots versus $1/n$ predict a crossing to limiting values of $\delta=87.5\pm0.3$ and 93 ± 1 ppm, respectively.

The remaining C≡C signals of **PtC$_x$Pt** cluster between $\delta=$ 67.9 and 55.3 ppm. Based upon assignments made for related dirhenium complexes,[11a] the PtC≡C*C* signals should have chemical shifts of $\delta=66$–67 ppm. The most upfield signal moves further upfield with increasing chain length, and a limiting value of $\delta=55.0\pm0.3$ ppm can be predicted for **PtC$_\infty$Pt**. Similar clusters of peaks in this region have been noted in all series of long conjugated polyynes characterized by ^{13}C NMR spectroscopy.[11a,13,34,39,43] Recent labeling studies suggest that the upfield signal is *not* associated with the innermost carbon atom.[34b] Therefore, the resonances of **PtC$_{28}$Pt** at $\delta=60$–63 ppm likely more closely model the chemical shift of the polyyne form of carbyne. The remaining C≡C signals of **PtC$_x$Si** exhibit analogous chemical shift phenomena.

UV/Vis spectra: The UV/Vis spectra of **PtC$_x$Pt** and **PtC$_x$Si** (Table 4 and Figure 1) exhibit distinctive chain-length effects. As found with all other series of long conjugated polyynes,[11a,13,24a,34,38,39,43,44] increasing numbers of progressively more intense bands are observed. Extinction coefficients (ε) of $>400\,000\,M^{-1}cm^{-1}$ are reached, and the deepening colors of the complexes are noted above. In all cases, particular care was taken with respect to sample purity. For **PtC$_{14}$Si**, **PtC$_{16}$Si**, and **PtC$_{20}$Si**, the quantities isolated were not suffi-

cient for accurate ε value determinations. Hence, the following analysis focuses on the diplatinum complexes **PtC$_x$Pt**.

A recent time-dependent DFT study of the model diplatinum complexes *trans*,*trans*-[$(C_6H_5)(H_3P)_2Pt(C{\equiv}C)_nPt(PH_3)_2(C_6H_5)$] ($n=2$, 3, 4, 5)[32] allows the principal electronic transitions in Figure 1 to be confidently assigned. Two $\pi\rightarrow\pi^*$ bands are predicted. The one at longer wavelength has predominant HOMO→LUMO character, but decreases markedly in intensity with increasing chain length. Only in the case of the C_4 complex is it computed to be more intense. The one at shorter wavelength is multiconfigurational, but with increasing chain length takes on more HOMO→LUMO character, and becomes dramatically more intense. Accordingly, the absorptions of **PtC$_x$Pt** at 489, 472, 444, 411, 371, 350, and 337 nm ($x=28$, 24, 20, 16, 12, 10, 8) are assigned to this transition (calcd for $x=10$ and 8,[32] 352 and 337 nm).[45]

In the case of **PtC$_8$Pt**, three much weaker bands appear at longer wavelengths than the most intense 337 nm band (359, 387, 419 nm, ε 17600–5600 $M^{-1}cm^{-1}$). These are believed to represent a vibrational progression of the other transition (calcd 446 nm). Analogous band patterns of the triethylsilyl-, methyl-, and phenyl-capped tetraynes $Et_3Si(C{\equiv}C)_4SiEt_3$, $Me(C{\equiv}C)_4Me$, and $Ph(C{\equiv}C)_4Ph$, respectively, have been similarly interpreted.[24a,34a,46] We have observed such fingerprints with all diplatinum octatetraynediyl complexes prepared to date.[13,14a] Complex **PtC$_{10}$Pt** exhibits three similar bands (391, 424, 462 nm), which are illustrated in Figure 5 (inset) and interpreted analogously. This pattern remains detectable with **PtC$_{12}$Pt** (420 sh, 455, 499 nm), but the lowest ε value is only 880 $M^{-1}cm^{-1}$, consistent with the prediction of diminishing intensities. Analogous bands could not be detected with **PtC$_{20}$Pt**.

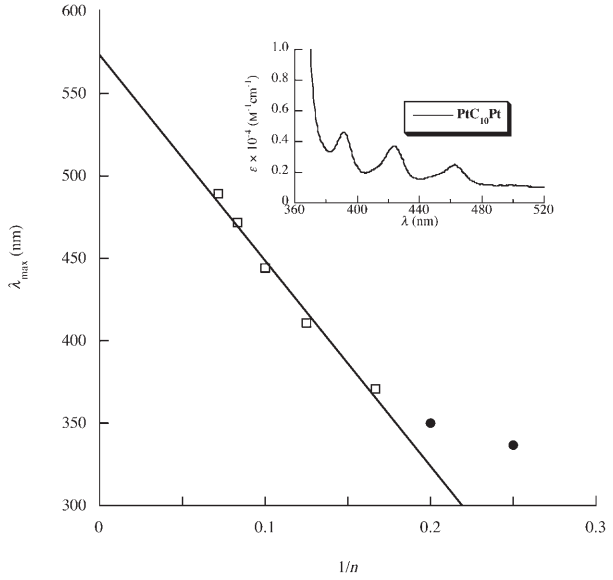

Figure 5. Relationship between λ_{max} values for the most intense UV/Vis absorptions of **PtC$_x$Pt** ($x \geq 8$) and $1/n$, in which n is the number of C≡C units. A representative extrapolation involving the complexes with the five longest chains is illustrated (R = 0.993). Inset: partial UV/Vis spectrum of **PtC$_{10}$Pt** showing the weak intensity longer wavelength bands.

The λ_{max} values for the most intense absorptions of **PtC$_8$Pt** through **PtC$_{28}$Pt** were plotted versus $1/n$. As shown in Figure 5, a good linear correlation was obtained for the five longest chain complexes (R = 0.993), giving a y intercept of 573 nm. Polynomial curve fittings involving all complexes or subsets thereof gave values somewhat greater than 600 nm. Other analytical methods for estimating such limits have recently been summarized.[47] Although 573 nm (or alternative extrapolated values) technically corresponds to the wavelength of the analogous transition in **PtC$_\infty$Pt**, computations establish that the amount of platinum character in the frontier orbitals will be negligible.[32] Hence, this should closely approximate the corresponding absorption of the polymer carbyne. UV/Vis data for most other series of polyynes X-$(C{\equiv}C)_n$X yield similar values (550–570 nm).[11a,34b,39,43] The analogous pentafluorophenyl complexes give a slightly lower limit (527–492 nm).[13]

These results constitute an experimental confirmation of a persistent, non-zero band gap for **PtC$_\infty$Pt** and hence carbyne. An absorption at 573 nm corresponds to a transition energy of 2.16 eV. However, it should be kept in mind that there remains another lower energy transition for **PtC$_x$Pt** and **PtC$_\infty$Pt**, but with a much smaller oscillator strength. Hence, the preceding treatment likely overestimates the true band gap and HOMO/LUMO energy difference. DFT computations on the model [$Pt(C{\equiv}C)_nPt$] compounds noted above predict a HOMO/LUMO gap of 1.49 eV (832 nm) for $n=8$.[13] Readers are referred to this study for further details regarding the electronic structure of these compounds.

Structures: The homologous series of structures **PtC$_6$Pt**, **Pt′C$_8$Pt′**, **PtC$_{10}$Pt**, and **PtC$_{12}$Pt** (Figure 3) complements the group of pentafluorophenyl C_6, C_8, C_{12}, and C_{16} analogues described earlier.[13] Together with the series **PtC$_4$Si**, **PtC$_6$Si**, **PtC$_8$Si**, and **PtC$_{10}$Si** (two pentafluorophenyl analogues of which have also been structurally characterized),[48] various effects of chain length upon structure can be examined. In general, the bond lengths and angles about platinum are unexceptional. However, there is a steady contraction of the Pt−C≡ bonds with chain length in both series. This can be reproduced computationally,[32] and detailed analyses show that this is due to increasing bond polarization, in line with the Brønsted acidity trends noted above. The chain becomes progressively more negative, and the platinum fragment positive, resulting in increased electrostatic attraction. Platinum/chain d–π* backbonding plays no significant role.

Computations also predict a number of trends regarding the C≡C and ≡C−C≡ bond lengths, such as increases in the former as the chain is lengthened or the midpoint is approached, and contractions in the latter.[32] However, the crystallographic data are usually not sufficiently accurate to verify these. The longest C≡C bond in Tables 6 and 7 (1.233(4) Å), and the shortest ≡C−C≡ bond (1.342 Å) are not quite at the limits predicted for the model for **PtC$_{26}$Pt** (1.242, 1.330 Å).[32] With regard to the other ligands, compu-

tations indicate that the Pt–C_{ipso} and Pt–P bonds should contract and lengthen, respectively. The former trend is suggested with **PtC$_x$Si** but not **PtC$_x$Pt**, whereas the latter is evident with **PtC$_x$Pt** but not **PtC$_x$Si**.

All of the new crystal structures show only a moderate degree of chain bending, as reflected by average bond angles in Tables 6 and 7, and further quantified with respect to other longer polyynes in a review.[4] For **PtC$_x$Pt**, the chain conformations are S-shaped; with the less symmetrical **PtC$_x$Si**, bow conformations are found. Although some compounds exhibit *p*-tolyl/*p*-tolyl/*p*-tolyl stacking interactions involving the phosphine ligands (e.g., **PtC$_6$Si** in Figure 2), the tendency is not as great as with the pentafluorophenyl analogues, in which additional attractive phenomena are in play.[13] Packing diagrams analogous to Figure 4 that illustrate features involving neighboring chains noted above are provided in the supporting information and elsewhere.[25]

Conclusions

Viable syntheses of the diplatinum sp carbon chain complexes **PtC$_6$Pt**, **PtC$_8$Pt**, **PtC$_{10}$Pt**, **PtC$_{12}$Pt**, **PtC$_{16}$Pt**, **PtC$_{20}$Pt**, **PtC$_{24}$Pt**, and **PtC$_{28}$Pt** have been developed. Although the yields and selectivities of some reactions can likely still be improved, reasonable quantities of these compounds can be accessed. For molecules with even numbers of C≡C linkages, the final step involves the oxidative homocoupling of **PtC$_{x/2}$H**. With **PtC$_{24}$Pt** and **PtC$_{28}$Pt**, it is critical to generate this labile precursor in the *presence* of the oxidizing agent (procedure C, Scheme 4). Although this methodology may eventually be limited by the competitive decomposition of **PtC$_{x/2}$H**, there is good reason to believe that it can be extended significantly beyond **PtC$_{14}$H**.

The thermal stabilities of these complexes often exceed 200 °C. **PtC$_{24}$Pt** and **PtC$_{28}$Pt** represent the first tetracosadodecayne and octacosatetradecayne that can be isolated in quantity and kept for extended periods at room temperature. There is no indication that any type of stability boundary has been reached. In contrast, organic polyynes with comparable (and often much lower) chain lengths rapidly decompose at room temperature, at least in the series investigated to date.

The spectroscopic and structural properties of **PtC$_x$Pt** establish a number of interesting chain-length effects. These are becoming increasingly well defined for polyynes. Hence, the value of future synthetic studies may increasingly lie more in the direction of applications, for example, macroscopic unsaturated connectors. Although polyynes are intrinsically reactive, they can also, at least when capped with platinum endgroups, be sterically shielded in much the manner of insulated household wire.[14] Efforts to elaborate the compounds reported herein to more complex assemblies,[49] as well as still longer C_x species, will be reported in due course.

Experimental Section

General: All reactions were conducted under dry nitrogen atmospheres by using conventional Schlenk techniques, but workups of platinum complexes were carried out in air. Solvents were treated as follows: THF, Et_2O, pentane, and hexane were distilled from Na/benzophenone; acetone was distilled from $CaCl_2$; CH_2Cl_2 was distilled from K_2CO_3; MeOH was distilled from Mg.

The following chemicals were used as purchased: *p*-tolMgBr (Aldrich, 1.0 M in Et_2O), acetyl chloride (generic label, technical), P(*p*-tol)$_3$ (≥97%, Fluka), $HNEt_2$ (≥99.5%, Fluka), HC≡CSiEt$_3$ (Aldrich), TMEDA (99%, Janssen), *n*Bu$_4$N$^+$F$^-$ (Aldrich, 1.0 M in THF/5 wt% H_2O), $ClSiMe_3$ (Lancaster), *n*BuLi (1.6 M in hexane, Acros), $ClSiEt_3$ (Lancaster), alumina for chromatography (neutral, Fluka). Other materials not listed were used as received from common commercial sources.

NMR spectra were obtained on modern 300–400 MHz spectrometers. IR and mass spectra were recorded on ASI React-IR 1000 and Micromass Zabspec instruments, respectively. DSC and TGA data were obtained with a Mettler-Toledo DSC-821 instrument.[31] Microanalyses were conducted on a Carlo Erba EA1110 instrument (in house) or by Atlantic Microlab.

[Pt(cod)(*p*-tol)$_2$]:[18] A Schlenk flask was charged with [$PtCl_2$(cod)] (2.005 g, 5.35 mmol)[17] and Et_2O (30 mL). Then *p*-tolMgBr (1.0 M in Et_2O; 13.4 mL, 13.4 mmol) was added with stirring. After 16 h, cold saturated aqueous NH_4Cl (25 mL) was added. The Et_2O phase was separated. The aqueous phase was extracted with Et_2O (3×50 mL). The combined Et_2O phases were dried ($MgSO_4$) and filtered through pads of Celite (1 cm) and decolorizing carbon (2 cm). The Et_2O was removed by rotary evaporation. The residue was suspended in EtOH (25 mL), collected by filtration, and dried by oil pump vacuum to give [Pt(cod)(*p*-tol)$_2$] as a white solid (1.685 g, 3.46 mmol, 65%). ^{1}H NMR ($CDCl_3$): δ = 7.11 (d, ^3J(H,H) = 7.8 Hz, ^3J(H,Pt) = 69.3 Hz, 4H; *o* to Pt), 6.83 (d, ^3J(H,H) = 7.3 Hz, 4H; *m* to Pt), 5.09 (s, ^2J(H,Pt) = 37.8 Hz, 4H; CH_2CH=), 2.50–2.37 (m, 8H; CH_2), 2.16 ppm (s, 6H; CH_3).

[PtCl(cod)(*p*-tol)]:[19] A Schlenk flask was charged with [Pt(cod)(*p*-tol)$_2$] (1.00 g, 2.06 mmol), CH_2Cl_2 (15 mL), and MeOH (15 mL). Acetyl chloride (0.24 mL, 3.4 mmol) was added with stirring. After 0.5 h, the solvent was removed by oil pump vacuum. The residue was suspended in MeOH (15 mL), collected by filtration, and dried by oil pump vacuum to give [PtCl(cod)(*p*-tol)] as a white solid (0.83 g, 1.9 mmol, 94%). ^{1}H NMR ($CDCl_3$): δ = 7.09 (d, ^3J(H,H) = 8.1 Hz, ^3J(H,Pt) = 40.5 Hz, 2H; *o* to Pt), 6.91 (d, ^3J(H,H) = 7.6 Hz, 2H; *m* to Pt), 5.78 (m, ^2J(H,Pt) = 24.4 Hz, 2H; CH_2CH=), 4.58 (m, ^2J(H,Pt) = 64.2 Hz, 2H; CH_2CH=), 2.67–2.29 (m, 8H; CH_2), 2.23 ppm (s, 3H; CH_3).

***trans*-[PtCl(*p*-tol){P(*p*-tol)$_3$}$_2$] (PtCl)**: A Schlenk flask was charged with [PtCl(cod)(*p*-tol)] (1.00 g, 2.33 mmol), P(*p*-tol)$_3$ (1.49 g, 4.89 mmol), and CH_2Cl_2 (30 mL). The mixture was stirred for 16 h. The solvent was removed by oil pump vacuum. The residue was suspended in MeOH (10 mL), collected by filtration, washed with hexane (2×3 mL), and dried by oil pump vacuum to give **PtCl** as a white solid (1.90 g, 1.91 mmol, 94%). Crystallization ($CHCl_3$/MeOH layer–layer diffusion) gave small white needles. M.p. 274 °C (decomp); elemental analysis calcd (%) for $C_{49}H_{49}ClP_2Pt$: C 67.44, H 5.34; found: C 67.10, H 5.23; ^{1}H NMR ($CDCl_3$): δ = 7.38–7.34 (m, 12H; *o* to P), 7.00 (d, ^3J(H,H) = 7.6 Hz, 12H; *m* to P), 6.40 (d, ^3J(H,H) = 8.1 Hz, 2H; *o* to Pt), 5.90 (d, ^3J(H,H) = 7.8 Hz, 2H; *m* to Pt), 2.29 (s, 18H; CH_3), 1.89 ppm (s, 3H; CH_3); ^{13}C{^{1}H} NMR ($CDCl_3$): δ = 139.6 (s, *p* to P), 136.8 (s, *o* to Pt), 135.1 (s, *i* to Pt), 134.7 (virtual t, ^2J(C,P) = 6.1 Hz, *o* to P),[20] 129.3 (s, *p* to Pt), 128.4 (s, *m* to P), 128.4 (s, *m* to Pt), 127.9 (virtual t, ^1J(C,P) = 26.0 Hz, *i* to P),[20] 21.4 (s, CH_3, *p* to P), 20.4 ppm (s, CH_3, *p* to Pt); ^{31}P{^{1}H} NMR ($CDCl_3$): δ = 22.9 (s, ^1J(P,Pt) = 3134 Hz).[50] MS:[51] *m*/*z* (%): 894 (34) [Pt(*p*-tol){P(*p*-tol)$_3$}$_2$]$^+$, 803 (100) [Pt{P(*p*-tol)$_3$}$_2$]$^+$, 497 (18) [Pt{P(*p*-tol)$_3$}]$^+$, 405 ppm (27) [Pt{P(*p*-tol)$_2$}], no other peaks above 400 of >5%.

***trans*-[Pt(*p*-tol){P(*p*-tol)$_3$}$_2${(C≡C)$_2$H}] (PtC$_4$H)**: A Schlenk flask was charged with **PtCl** (1.00 g, 1.08 mmol), CuI (0.025 g, 0.13 mmol), and $HNEt_2$ (50 mL), and cooled to −45 °C (CO_2/CH_3CN). Then H(C≡C)$_2$H (2.14 M in THF, 13.6 mL, 29.1 mmol)[21] was added with stirring. After 1 h,

the cold bath was removed. After 1 h, the solvent was removed by rotary evaporation. The residue was extracted with toluene (4×25 mL). The extracts were filtered through an alumina column (3×7 cm). The toluene was removed by rotary evaporation. The residue was suspended in MeOH (10 mL), collected by filtration, and dried by oil pump vacuum to give **PtC_4H** as a pale tan powder (0.83 g, 0.88 mmol, 82%). The sample slightly darkened at 155°C, slowly turned black with further heating, and liquefied at 180°C (capillary). DSC/TGA data: Table 1; elemental analysis calcd (%) for $C_{53}H_{50}P_2Pt$: C 67.43, H 5.34; found (two samples): C 67.34/67.10, H 5.43/5.23; ^{1}H NMR ($CDCl_3$): δ=7.36–7.31 (m, 12H; *o* to P), 7.01 (d, ^3J(H,H)=7.8 Hz, 12H; *m* to P), 6.28 (d, ^3J(H,H)=7.8 Hz, 2H; *o* to Pt), 6.02 (d, ^3J(H,H)=7.6 Hz, 2H; *m* to Pt), 2.30 (s, 18H; CH_3), 1.92 (s, 3H; CH_3), 1.41 ppm (s, 1H; ≡CH); ^{13}C{^{1}H} NMR ($CDCl_3$): δ= 150.5 (t, ^2J(C,P)=10.3 Hz, *i* to Pt), 139.7 (s, *p* to P), 138.8 (s, *o* to Pt), 134.6 (virtual t, ^2J(C,P)=6.1 Hz, *o* to P),[20] 129.2 (s, *p* to Pt), 129.0 (s, *m* to P), 128.3 (virtual t, ^1J(C,P)=28.9 Hz, *i* to P),[20] 128.1 (s, *m* to Pt), 110.6 (t, ^2J(C,P)=13.8 Hz, ^1J(C,Pt)=650 Hz,[50] PtC≡C), 95.3 (s, ^2J-(C,Pt)=225 Hz,[50] PtC≡*C*), 72.9 (s, *C*≡CH), 58.1 (s, C≡*C*H), 21.3 (s, *C*H_3, *p* to P), 20.6 ppm (s, *C*H_3, *p* to Pt); ^{13}C NMR ($CDCl_3$, no ^{1}H decoupling): δ=151.2 (t, ^2J(C,P)=10.3 Hz, *i* to Pt), 140.4–140.3 (m, *p* to P), 139.5 (dd, ^1J(C,H)=160.9 Hz, ^2J(C,H)=6.9 Hz, *o* to Pt), 135.3 (dd, ^1J(C,H)= 160.9 Hz, ^2J(C,H)=6.9 Hz, *o* to P), 129.9 (s, *p* to Pt), 129.0 (dt, ^1J(C,H)= 157.9 Hz, ^2J(C,H)=10.6 Hz, *m* to P), 128.8 (m, *i* to P), 128.3 (m, *m* to Pt), 111.2 (t, ^2J(C,P)=13.8 Hz, ^1J(C,Pt)=650 Hz,[50] PtC≡C), 96.0 (d, ^3J-(C,H)=5.2 Hz, ^2J(C,Pt)=225 Hz,[50] PtC≡*C*), 73.6 (d, ^2J(C,H)=50.9 Hz, *C*≡CH), 58.8 (d, ^1J(C,H)=249.6 Hz, C≡*C*H), 22.0 (qt, ^1J(C,H)=125.7 Hz, ^3J(C,H)=4.2 Hz, *C*H_3, *p* to P), 21.2 ppm (qt, ^1J(C,H)=125.0 Hz, ^3J-(C,H)=4.2 Hz, *C*H_3, *p* to Pt); ^{31}P{^{1}H} NMR ($CDCl_3$): δ=19.4 ppm (s, ^1J-(P,Pt)=2939 Hz);[50] IR data: Table 2; UV/Vis data: Table 4; MS:[51] *m*/*z* (%): 944 (8) [**PtC_4H**]$^+$, 894 (30) [Pt(*p*-tol){P(*p*-tol)$_3$}$_2$]$^+$, 803 (100) [Pt{P-(*p*-tol)$_3$}$_2$]$^+$, 497 (24) [Pt{P(*p*-tol)$_3$}]$^+$, 405 (34) [Pt{P(*p*-tol)$_2$}]$^+$, no other peaks above 400 of >7%.

***trans*-[Pt(*p*-tol){P(*p*-tol)$_3$}$_2${(C≡C)$_3$SiEt$_3$}] (PtC_6Si)**: A three-necked flask was charged with **PtC_4H** (0.330 g, 0.350 mmol), HC≡CSiEt_3 (0.566 g, 11.2 mmol), and acetone (40 mL), and fitted with a gas dispersion tube and a condenser.[52] A Schlenk flask was charged with CuCl (0.200 g, 2.04 mmol) and acetone (20 mL), and TMEDA (0.200 mL, 1.33 mmol) was added with stirring. After 0.5 h, stirring was halted, and a grayish solid separated from a blue supernatant. Then O_2 was bubbled through the three-necked flask with stirring. After about 5 min, the blue supernatant was added in portions. After 1 h, the solvent was removed by rotary evaporation. The residue was extracted with hexane (3×10 mL) and then toluene (3×25 mL). The extracts were passed in sequence through an alumina column (2×7 cm). The solvent was removed from the toluene extracts by rotary evaporation. The residue was subjected to chromatography on a silica gel column (2.5×25 cm, packed in hexane, eluted with 15:85 v/v CH_2Cl_2/hexane). The solvent was removed from the product-containing fraction by rotary evaporation and dried by oil pump vacuum to give **PtC_6Si** as a yellow solid (0.299 g, 0.268 mmol, 77%). DSC/TGA data: Table 1; elemental analysis calcd (%) for $C_{61}H_{64}P_2PtSi$: C 67.70, H 5.96; found: C 67.24, H 5.95; ^{1}H NMR ($CDCl_3$): δ=7.32–7.27 (m, 12H; *o* to P), 7.00 (d, ^3J(H,H)=7.7 Hz, 12H; *m* to P), 6.26 (d, ^3J(H,H)=8.3 Hz, 2H; *o* to Pt), 6.04 (d, ^3J(H,H)=7.7 Hz, 2H; *m* to Pt), 2.31 (s, 18H; CH_3), 1.92 (s, 3H; CH_3), 0.91 (t, ^3J(H,H)=8.0 Hz, 9H; CH_2CH_3), 0.51 ppm (q, ^3J(H,H)=7.9 Hz, 6H; CH_2CH_3); ^{13}C{^{1}H} NMR ($CDCl_3$): δ=150.2 (t, ^2J-(C,P)=9.9 Hz, *i* to Pt), 139.9 (s, *p* to P), 138.7 (s, *o* to Pt), 134.5 (virtual t, ^2J(C,P)=6.9 Hz, *o* to P),[20] 129.3 (s, *p* to Pt), 128.4 (virtual t, ^2J(C,P)= 5.4 Hz, *m* to P),[20] 127.8 (virtual t, ^1J(C,P)=20.1 Hz, *i* to P),[20] 127.5 (s, *m* to Pt), 117.5 (t, ^2J(C,P)=14.8 Hz, ^1J(C,Pt)=838 Hz,[50] PtC≡C), 95.8 (s, ^2J-(C,Pt)=212 Hz,[50] PtC≡*C*), 91.8 (s, *C*≡CSi), 79.1 (s, C≡CSi), 66.6 (s, PtC≡ C*C*≡C), 54.9 (s, PtC≡CC≡*C*), 21.3 (s, *C*H_3, *p* to P), 20.6 (s, *C*H_3, *p* to Pt), 7.4 (s, 3CH_2CH_3), 4.4 ppm (s, 3CH_2CH_3); ^{31}P{^{1}H} NMR ($CDCl_3$): δ= 19.5 ppm (s, ^1J(P,Pt)=2921 Hz);[50] IR data: Table 2; UV/Vis data: Table 4; MS:[51] *m*/*z* (%): 1081 (4) [**PtC_6Si**]$^+$, 990 (4) [PtC_6SiEt_3{P(*p*-tol)$_3$}$_2$]$^+$, 894 (24) [Pt(*p*-tol){P(*p*-tol)$_3$}$_2$]$^+$, 803 (100) [Pt{P(*p*-tol)$_3$}$_2$]$^+$, 497 (20) [Pt{P(*p*-tol)$_3$}]$^+$, 405 (27) [Pt{P(*p*-tol)$_2$}]$^+$, no other peaks above 400 of >7%.

***trans*-[Pt(*p*-tol){P(*p*-tol)$_3$}$_2${(C≡C)$_3$H}] (PtC_6H)**: A Schlenk flask was charged with **PtC_6Si** (0.400 g, 0.370 mmol) and THF (50 mL). Then wet nBu$_4$N$^+$F$^-$ (1.0 M in THF/5 wt% H_2O; 0.050 mL, 0.050 mmol) was added with stirring. After 0.5 h, the mixture was poured into water (40 mL) and extracted with CH_2Cl_2 (3×30 mL). The combined extracts were dried ($MgSO_4$), and the solvent was removed by rotary evaporation while cooling the sample in an ice bath. The residue was extracted with hexane (3× 10 mL), which was passed through a silica gel column (2×15 cm) and discarded. The residue was extracted with CH_2Cl_2 (3×2 mL), which was passed through the same column using 10:90 v/v CH_2Cl_2/hexane. The solvent was removed by oil pump vacuum at 0°C to give **PtC_6H** as a white solid (0.301 g, 0.311 mmol, 84%), m.p. 135°C (decomp). This compound darkens at room temperature within a few minutes, but can be stored without discolorization at −24°C for several days. ^{1}H NMR ($CDCl_3$): δ= 7.31–7.27 (m, 12H; *o* to P), 7.01 (d, ^3J(H,H)=7.8 Hz, 12H; *m* to P), 6.27 (d, ^3J(H,H)=7.8 Hz, 2H; *o* to Pt), 6.04 (d, ^3J(H,H)=7.6 Hz, 2H; *m* to Pt), 2.31 (s, 18H; CH_3), 1.93 (s, 3H; CH_3), 1.79 ppm (s, 1H; ≡CH); ^{13}C{^{1}H} NMR ($CDCl_3$): δ=150.6 (t, ^2J(C,P)=10 Hz, *i* to Pt), 140.6 (s, *p* to P), 139.4 (s, *o* to Pt), 135.2 (virtual t, ^2J(C,P)=6.2 Hz, *o* to P),[20] 130.1 (s, *p* to Pt), 129.0 (virtual t, ^3J(C,P)=5.2 Hz, *m* to P),[20] 128.9 (s, *m* to Pt), 128.4 (virtual t, ^1J(C,P)=29.2 Hz, *i* to P),[20] 117.4 (t, ^2J(C,P)=14.5 Hz, ^1J-(C,Pt)=875 Hz,[50] Pt*C*≡C), 96.0 (s, ^2J(C,Pt)=238 Hz,[50] PtC≡*C*), 71.5 (s, *C*≡CH), 66.0 (s, PtC≡C*C*≡C), 64.7 (s, C≡*C*H), 54.8 (s, PtC≡CC≡*C*), 22.0 (s, *C*H_3, *p* to P), 21.2 ppm (s, *C*H_3, *p* to Pt); ^{13}C NMR ($CDCl_3$, no ^{1}H decoupling): δ=150.6 (t, ^2J(C,P)=10.0 Hz, *i* to Pt), 140.7–140.5 (m, *p* to P), 139.5 (dd, ^1J(C,H)=153.2 Hz, ^2J(C,H)=9.1 Hz, *o* to Pt), 135.2 (dd, ^1J-(C,H)=160.9 Hz, ^2J(C,H)=6.1 Hz, *o* to P), 130.1–130.0 (m, *p* to Pt), 129.0–129.6 (m, *m* to P), 128.7–128.6 (m, *m* to Pt), 128.4 (m, *i* to P), 117.2 (t, ^2J(C,P)=14.5 Hz, ^1J(C,Pt)=875 Hz,[50] Pt*C*≡C), 96.1 (s, ^2J(C,Pt)= 238 Hz,[50] PtC≡*C*), 71.5 (d, ^2J(C,H)=51.6 Hz, *C*≡CH), 66.0 (s, PtC≡C*C*≡ C), 64.7 (d, ^1J(C,H)=255.0 Hz, C≡*C*H), 54.8 (d, ^3J(C,H)=6.8 Hz, PtC≡ C*C*≡*C*), 22.0 (qt, ^1J(C,H)=126.0 Hz, ^3J(C,H)=4.5 Hz, *C*H_3, *p* to P), 21.2 ppm (qt, ^1J(C,H)=124.5 Hz, ^3J(C,H)=4.9 Hz, *C*H_3, *p* to Pt); ^{31}P{^{1}H} NMR ($CDCl_3$): δ=19.1 ppm (s, ^1J(P,Pt)=2906 Hz).[50] IR data: Table 2.

***trans*-[Pt(*p*-tol){P(*p*-tol)$_3$}$_2${(C≡C)$_4$SiEt$_3$}] (PtC_8Si)**: A Schlenk flask was charged with **PtC_6Si** (0.216 g, 0.200 mmol) and THF (25 mL). Then wet nBu$_4$N$^+$F$^-$ (1.0 M in THF/5 wt% H_2O, 0.025 mL, 0.025 mmol) was added with stirring. After 0.5 h (TLC showed no reactant remaining), the mixture was poured into water (20 mL) and extracted with CH_2Cl_2 (3× 20 mL). The combined extracts were dried ($MgSO_4$). The solvent was removed by rotary evaporation while cooling the sample in an ice bath. The residue was extracted with hexane (3×10 mL), which was passed through a silica gel column (3×15 cm) and discarded. The residue was subjected to chromatography on the same column using 15:85 v/v CH_2Cl_2/hexane. The solvent was removed from the eluate by rotary evaporation (ice bath). The residue was dissolved in acetone (30 mL) and transferred to a three-necked flask, which was fitted with a gas dispersion tube and a condenser.[52] Then HC≡CSiEt_3 (0.556 g, 11.21 mmol) was added. A Schlenk flask was charged with CuCl (0.200 g, 0.204 mmol) and acetone (20 mL), and TMEDA (0.200 mL, 1.33 mmol) was added with stirring. After 0.5 h, stirring was halted, and a grayish solid separated from a blue supernatant. Then O_2 was bubbled through the three-necked flask with stirring. After about 5 min, the blue supernatant was added in portions. After 1.5 h, the solvent was removed by rotary evaporation. The residue was extracted with hexane and then toluene. The extracts were passed in sequence through an alumina column (2×7 cm). The solvent was removed from the toluene extracts by rotary evaporation. The residue was subjected to chromatography on a silica gel column (3× 30 cm, packed with hexane). Elution with 15:85 v/v CH_2Cl_2/hexane gave **PtC_8Si**, and 30:70 v/v CH_2Cl_2/hexane gave **$PtC_{12}Pt$**. The solvent was removed from each band by oil pump vacuum to give **PtC_8Si** as a yellow solid (0.050 g, 0.045 mmol, 23%), and **$PtC_{12}Pt$** as a bright orange powder described below (0.073 g, 0.038 mmol, 38%). DSC/TGA, Table 1; elemental analysis calcd (%) for $C_{63}H_{64}P_2PtSi$: C 68.40, H 5.83; found: C 67.87, H 5.82; ^{1}H NMR ($CDCl_3$): δ=7.31–7.26 (m, 12H; *o* to P), 7.02 (d, ^3J(H,H)=7.7 Hz, 12H; *m* to P), 6.16 (d, ^3J(H,H)=7.7 Hz, 2H; *o* to Pt), 6.07 (d, ^3J(H,H)=7.7 Hz, 2H; *m* to Pt), 2.32 (s, 18H; CH_3), 1.94 (s, 3H; CH_3), 0.97 (t, ^3J(H,H)=8.0 Hz, 9H; CH_2CH_3), 0.58 ppm (q, ^3J(H,H)= 8.3 Hz, 6H; CH_2CH_3); ^{13}C{^{1}H} NMR ($CDCl_3$): δ=149.5 (t, ^2J(C,P)= 9.9 Hz, *i* to Pt), 140.0 (s, *p* to P), 138.7 (s, *o* to Pt), 134.5 (virtual t, ^2J-(C,P)=6.1 Hz, *o* to P),[20] 129.5 (s, *p* to Pt), 128.4 (virtual t, ^3J(C,P)=

5.3 Hz, *m* to P),[20] 127.7 (s, *m* to Pt), 127.6 (virtual t, ^1J(C,P) = 29.0 Hz, *i* to P),[20] 120.4 (t, ^2J(C,P) = 13.6 Hz, Pt*C*≡C), 95.6 (s, PtC≡*C*), 90.6 (s, C≡*C*Si), 81.9 (s, *C*≡CSi), 67.0, 64.8, 58.4, 55.1, (4 s, PtC≡*C*C≡*C*C≡*C*), 21.4 (s, *C*H$_3$, *p* to P), 20.5 (s, *C*H$_3$, *p* to Pt), 7.3 (s, CH$_2$*C*H$_3$), 4.2 ppm (s, *C*H$_2$CH$_3$); ^{31}P{^{1}H} NMR (CDCl$_3$): δ = 19.2 ppm (s, ^1J(P,Pt) = 2902 Hz);[50] IR data: Table 2; UV/Vis data: Table 4; MS:[51] *m*/*z* (%): 1105 (2) [**PtC$_8$Si**]$^+$, 894 (12) [Pt(*p*-tol){P(*p*-tol)$_3$}$_2$]$^+$), 803 (100) [Pt{P(*p*-tol)$_3$}$_2$]$^+$, 497 (36) [Pt{P(*p*-tol)$_3$}]$^+$, 405 (62) [Pt{P(*p*-tol)$_2$}]$^+$.

***trans*-[Pt(*p*-tol){P(*p*-tol)$_3$}$_2${(C≡C)$_6$SiEt$_3$}] (PtC$_{12}$Si)**: A three-necked flask was charged with **PtC$_8$Si** (0.150 g, 0.136 mmol) and acetone (35 mL), and fitted with a gas dispersion tube and a condenser.[52] Then wet *n*Bu$_4$N$^+$F$^-$ (1.0 M in THF/5 wt% H$_2$O, 0.050 mL, 0.050 mmol) was added with stirring. After 0.5 h (TLC showed no reactant remaining), Me$_3$SiCl (0.025 mL, 0.20 mmol) was added; after 10 min, H(C≡C)$_2$SiEt$_3$ (0.447 g, 2.72 mmol) was added. A Schlenk flask was charged with CuCl (0.218 g, 2.21 mmol) and acetone (10 mL), and TMEDA (0.200 mL, 1.33 mmol) was added with stirring. After 0.5 h, stirring was halted, and a grayish solid separated from a blue supernatant. Then O$_2$ was bubbled through the three-necked flask with stirring and the blue supernatant was added in portions. After 1.5 h, the solvent was removed by rotary evaporation. The residue was extracted with hexane (3×30 mL) and toluene (3×40 mL). The extracts were passed in sequence through an alumina column (2×10 cm). The solvent was removed from the toluene extracts by rotary evaporation and the residue was subjected to chromatography on a silica gel column (3.5×40 cm, packed in hexane, eluted with 15:85 v/v CH$_2$Cl$_2$/hexane). The solvent was removed from the product-containing fractions by rotary evaporation and oil pump vacuum to give **PtC$_{12}$Si** as an orange solid (0.066 g, 0.057 mmol, 42%). DSC/TGA data: Table 1; elemental analysis calcd (%) for C$_{67}$H$_{64}$P$_2$PtSi: C 69.71, H 5.59; found: C 69.35, H 5.73. ^{1}H NMR (CDCl$_3$): δ = 7.29–7.24 (m, 12H; *o* to P), 7.02 (d, ^3J(H,H) = 7.8 Hz, 12H; *m* to P), 6.26 (d, ^3J(H,H) = 7.8 Hz, 2H; *o* to Pt), 6.07 (d, ^3J(H,H) = 7.7 Hz, 2H; *m* to Pt), 2.32 (s, 18H; CH$_3$), 1.94 (s, 3H; CH$_3$), 0.97 (t, ^3J(H,H) = 7.9 Hz, 9H; CH$_2$C*H*$_3$), 0.58 ppm (q, ^3J(H,H) = 7.9 Hz, 6H; C*H*$_2$CH$_3$); ^{13}C{^{1}H} NMR (CDCl$_3$): δ = 149.2 (t, ^2J(C,P) = 10.2 Hz, *i* to Pt), 140.1 (s, *p* to P), 138.6 (s, *o* to Pt), 134.5 (virtual t, ^2J(C,P) = 6.0 Hz, *o* to P),[20] 129.7 (s, *p* to Pt), 128.5 (virtual t, ^3J(C,P) = 5.5 Hz, *m* to P),[20] 127.8 (s, *m* to Pt), 127.5 (virtual t, ^1J(C,P) = 29.6 Hz, *i* to P),[20] 123.7 (t, ^2J(C,P) = 13.9 Hz, Pt*C*≡C), 95.3 (s, PtC≡*C*), 89.4 (s, C≡*C*Si), 85.5 (s, *C*≡CSi), 67.4, 66.0, 64.4, 62.8, 60.9, 60.1, 58.9, 55.3 (8 s, PtC≡*C*C≡*C*C≡*C*C≡*C*C≡*C*), 21.4 (s, *C*H$_3$, *p* to P), 20.5 (s, *C*H$_3$, *p* to Pt), 7.3 (s, CH$_2$*C*H$_3$), 4.2 ppm (s, *C*H$_2$CH$_3$); ^{31}P{^{1}H} NMR (CDCl$_3$): δ = 19.0 ppm (s, ^1J(P,Pt) = 2892 Hz);[50] IR data: Table 2; UV/Vis data: Table 4; MS:[51] *m*/*z* (%): 1153 (2) [**PtC$_{12}$Si**]$^+$, 894 (20) [Pt(*p*-tol){P(*p*-tol)$_3$}$_2$]$^+$), 803 (100) [Pt{P(*p*-tol)$_3$}$_2$]$^+$, 497 (36) [Pt{P(*p*-tol)$_3$}]$^+$, 405 (58) [Pt{P(*p*-tol)$_2$}]$^+$.

Reaction of PtC$_4$H and H(C≡C)$_2$SiEt$_3$ (PtC$_8$Si, PtC$_{12}$Si, PtC$_{16}$Si): A three-necked flask was charged with **PtC$_4$H** (0.260 g, 0.275 mmol) and acetone (40 mL), and fitted with a gas dispersion tube and a condenser.[52] A Schlenk flask was charged with CuCl (0.200 g, 0.204 mmol) and acetone (20 mL), and TMEDA (0.400 mL, 2.67 mmol) was added with stirring. After 0.5 h, stirring was halted, and a grayish solid separated from a blue supernatant. Then O$_2$ was bubbled through the three-necked flask with stirring. After about 5 min, H(C≡C)$_2$SiEt$_3$ (0.905 g, 5.51 mmol) was added, followed by the blue supernatant in portions. After 1.5 h, the solvent was removed by rotary evaporation. The residue was extracted first with hexane (3×25 mL) and then with toluene (3×30 mL). The extracts were passed in sequence through an alumina column (2×7 cm). The solvent was removed from the toluene extracts by rotary evaporation. The residue was subjected to chromatography on a silica gel column (3.5×40 cm, packed in hexane, eluted with 15:85 v/v CH$_2$Cl$_2$/hexane). The solvent was removed from the product-containing fractions by rotary evaporation and oil pump vacuum to give **PtC$_{16}$Si** as a deep red solid (0.004 g, 0.003 mmol, 1%), **PtC$_{12}$Si** as an orange solid (0.102 g, 0.0880 mmol, 30%), and **PtC$_8$Si** as a yellow solid (0.088 g, 0.080 mmol, 29%). Data for **PtC$_{16}$Si**: m.p. 104 °C (decomp); elemental analysis calcd (%) for C$_{71}$H$_{64}$P$_2$PtSi: C 70.86, H 5.44; found: C 69.82, H 5.62; ^{1}H NMR (CDCl$_3$): δ = 7.29–7.24 (m, 12H; *o* to P), 7.02 (*d*, ^3J(H,H) = 7.7 Hz, 12H; *m* to P), 6.25 (d, ^3J(H,H) = 7.7 Hz, 2H; *o* to Pt), 6.07 (d, ^3J(H,H) = 7.6 Hz, 2H; *m* to Pt), 2.32 (s, 18H; CH$_3$), 1.94 (s, 3H; CH$_3$), 0.97 (t, ^3J(H,H) = 8.4 Hz, 9H; CH$_2$C*H*$_3$), 0.62 ppm (q, ^3J(H,H) = 7.9 Hz, 6H; C*H*$_2$CH$_3$); ^{13}C{^{1}H} NMR (CDCl$_3$): δ = 149.1 (t, ^2J(C,P) = 9.9 Hz, *i* to Pt), 140.2 (s, *p* to P), 138.6 (s, *o* to Pt), 134.5 (virtual t, ^2J(C,P) = 6.1 Hz, *o* to P),[20] 129.8 (s, *p* to Pt), 128.5 (virtual t, ^3J(C,P) = 5.3 Hz, *m* to P),[20] 127.8 (s, *m* to Pt), 127.4 (virtual t, ^1J(C,P) = 30.3 Hz, *i* to P),[20] 125.2 (t, ^2J(C,P) = 14.5 Hz, Pt*C*≡C), 95.1 (s, PtC≡*C*), 88.9 (s, C≡*C*Si), 87.1 (s, *C*≡CSi), 67.9, 66.6, 65.0, 63.9, 63.1, 62.1, 62.0 (two coincident signals), 61.2, 60.1, 58.8, 55.4 (11 s, PtC≡*C*C≡*C*C≡*C*C≡*C*C≡*C*C≡*C*), 21.4 (s, *C*H$_3$, *p* to P), 20.5 (s, *C*H$_3$, *p* to Pt), 7.3 (s, CH$_2$*C*H$_3$), 4.0 ppm (s, *C*H$_2$CH$_3$); ^{31}P{^{1}H} NMR (CDCl$_3$): δ = 19.0 ppm (s, ^1J(P,Pt) = 2889 Hz);[50] IR data: Table 2; UV/Vis data: Table 4; MS:[51] *m*/*z* (%): 1201 (1) [**PtC$_{16}$Si**]$^+$, 894 (35) [Pt(*p*-tol){P(*p*-tol)$_3$}$_2$]$^+$, 803 (100) [Pt{P(*p*-tol)$_3$}$_2$]$^+$, 497 (36) [Pt{P(*p*-tol)$_3$}]$^+$, 405 (54) [Pt{P(*p*-tol)$_2$}]$^+$.

Reaction of PtC$_6$H and H(C≡C)$_2$SiEt$_3$ (PtC$_{10}$Si, PtC$_{14}$Si): A three-necked flask was charged with **PtC$_6$Si** (0.216 g, 0.200 mmol) and acetone (40 mL), and fitted with a gas dispersion tube and a condenser.[52] Then wet *n*Bu$_4$N$^+$F$^-$ (1.0 M in THF/5 wt% H$_2$O, 0.050 mL, 0.050 mmol) was added with stirring. After 0.5 h (TLC showed no reactant remaining), Me$_3$SiCl (0.025 mL, 0.20 mmol) was added; after 10 min, H(C≡C)$_2$SiEt$_3$ (0.657 g, 4.00 mmol) was added. A Schlenk flask was charged with CuCl (0.218 g, 2.21 mmol) and acetone (20 mL), and TMEDA (0.200 mL, 1.33 mmol) was added with stirring. After 0.5 h, stirring was halted, and a grayish solid separated from a blue supernatant. Then O$_2$ was bubbled through the three-necked flask with stirring. After about 5 min, the blue supernatant was added in portions. After 1.5 h, the solvent was removed by rotary evaporation. The residue was extracted with hexane (3×30 mL) and toluene (3×40 mL). The extracts were passed in sequence through an alumina column (2×10 cm). The solvent was removed from toluene extracts by rotary evaporation and the residue was subjected to chromatography on a silica gel column (3.5×40 cm, packed in hexane, eluted with 15:85 v/v CH$_2$Cl$_2$/hexane). The solvent was removed from the product-containing fractions by rotary evaporation and oil pump vacuum to give **PtC$_{14}$Si** as a red solid described below (0.016 g, 0.014 mmol, 7%) and **PtC$_{10}$Si** as an orange solid (0.134 g, 0.118 mmol, 59%). Data for **PtC$_{10}$Si**: DSC/TGA, Table 1; elemental analysis calcd (%) for C$_{65}$H$_{64}$P$_2$PtSi: C 69.07, H 5.71; found: C 68.75, H 5.80; ^{1}H NMR (CDCl$_3$): δ = 7.30–7.25 (m, 12H; *o* to P), 7.02 (d, ^3J(H,H) = 7.7 Hz, 12H; *m* to P), 6.26 (d, ^3J(H,H) = 7.9 Hz, 2H; *o* to Pt), 6.07 (d, ^3J(H,H) = 7.7 Hz, 2H; *m* to Pt), 2.32 (s, 18H; CH$_3$), 1.94 (s, 3H; CH$_3$), 0.95 (t, ^3J(H,H) = 7.9 Hz, 9H; CH$_2$C*H*$_3$), 0.59 ppm (q, ^3J(H,H) = 7.8 Hz, 6H; C*H*$_2$CH$_3$); ^{13}C{^{1}H} NMR (CDCl$_3$): δ = 149.4 (t, ^2J(C,P) = 10.2 Hz, *i* to Pt), 140.1 (s, *p* to P), 138.6 (s, *o* to Pt), 134.5 (virtual t, ^2J(C,P) = 6.0 Hz, *o* to P),[20] 129.6 (s, *p* to Pt), 128.3 (virtual t, ^3J(C,P) = 5.1 Hz, *m* to P),[20] 128.1 (s, *m* to Pt), 127.5 (virtual t, ^1J(C,P) = 27.3 Hz, *i* to P),[20] 122.4 (t, ^2J(C,P) = 14.8 Hz, Pt*C*≡C), 95.4 (s, PtC≡*C*), 89.8 (s, C≡*C*Si), 84.1 (s, *C*≡CSi), 67.1, 65.6, 63.5, 59.7, 58.7, 55.3 (6 s, PtC≡*C*C≡*C*C≡*C*C≡*C*C≡*C*), 21.4 (s, *C*H$_3$, *p* to P), 20.5 (s, *C*H$_3$, *p* to Pt), 7.3 (s, *C*H$_2$CH$_3$), 4.1 ppm (s, CH$_2$*C*H$_3$); ^{31}P{^{1}H} NMR (CDCl$_3$): δ = 19.1 ppm (s, ^1J(P,Pt) = 2898 Hz);[50] IR data: Table 2; UV/Vis data: Table 4; MS:[51] *m*/*z* (%): 1129 (<1) [**PtC$_{10}$Si**]$^+$, 894 (22) [Pt(*p*-tol){P(*p*-tol)$_3$}$_2$]$^+$, 803 (100) [Pt{P(*p*-tol)$_3$}$_2$]$^+$, 497 (31) [Pt{P(*p*-tol)$_3$}]$^+$, 405 (44) [Pt{P(*p*-tol)$_2$}]$^+$.

***trans*-[Pt(*p*-tol){P(*p*-tol)$_3$}$_2${(C≡C)$_7$SiEt$_3$}] (PtC$_{14}$Si)**: A three-necked flask was charged with **PtC$_{10}$Si** (0.150 g, 0.133 mmol) and acetone (20 mL), fitted with a gas dispersion tube and a condenser, and cooled to 0 °C. Then wet *n*Bu$_4$N$^+$F$^-$ (1.0 M in THF/5 wt% H$_2$O, 0.100 mL, 0.100 mmol) was added with stirring. After 0.5 h (TLC showed no reactant remaining), Me$_3$SiCl (0.050 mL, 0.40 mmol) was added; after 10 min, H(C≡C)$_2$SiEt$_3$ (0.437 g, 2.66 mmol) was added. A Schlenk flask was charged with CuCl (0.436 g, 4.42 mmol) and acetone (5 mL), and TMEDA (0.400 mL, 2.66 mmol) was added with stirring. After 0.5 h, stirring was halted, and a grayish solid separated from a blue supernatant. The blue supernatant was added to the three-necked flask. Then O$_2$ was bubbled through the three-necked flask with stirring. After 1.5 h, the solvent was removed by rotary evaporation. The residue was extracted first with hexane (3×30 mL) and then with toluene (3×40 mL). The extracts were passed in sequence through an alumina column (2×10 cm, packed in hexane). The solvent was removed from toluene extracts by rotary evaporation and the residue was subjected to chromatography on a silica gel column (3.5×40 cm, packed in hexane, eluted with 15:85 v/v CH$_2$Cl$_2$/hexane). The solvent was removed from the product-containing fraction by rotary evapo-

ration and oil pump vacuum to give **$PtC_{14}Si$** as a red solid (0.031 g, 0.026 mmol, 20%). DSC/TGA data: Table 1; elemental analysis calcd (%) for $C_{69}H_{64}P_2PtSi$: C 70.33, H 5.47; found: C 69.59, H 5.52; ^{1}H NMR ($CDCl_3$): δ = 7.29–7.26 (m, 12H; *o* to P), 7.02 (*d*, ^3J(H,H) = 7.7 Hz, 12H; *m* to P), 6.25 (d, ^3J(H,H) = 7.8 Hz, 2H; *o* to Pt), 6.07 (*d*, ^3J(H,H) = 7.7 Hz, 2H; *m* to Pt), 2.32 (s, 18H; CH_3), 1.94 (s, 3H; CH_3), 0.97 (t, ^3J(H,H) = 7.9 Hz, 9H; CH_2CH_3), 0.62 ppm (q, ^3J(H,H) = 7.9 Hz, 6H; CH_2CH_3); $^{13}C\{^1H\}$ NMR ($CDCl_3$): δ = 149.2 (t, ^2J(C,P) = 9.7 Hz, *i* to Pt), 140.1 (s, *p* to P), 138.6 (s, *o* to Pt), 134.5 (virtual t, ^2J(C,P) = 6.0 Hz, *o* to P),[20] 129.7 (s, *p* to Pt), 128.5 (virtual t, ^3J(C,P) = 5.5 Hz, *m* to P),[20] 127.9 (s, *m* to Pt), 127.5 (virtual t, ^1J(C,P) = 29.6 Hz, *i* to P),[20] 124.6 (t, ^2J(C,P) = 14.3 Hz, PtC≡C), 95.2 (s, PtC≡*C*), 89.1 (s, C≡*C*Si), 86.5 (s, *C*≡CSi), 67.6, 66.3, 64.7, 63.6, 62.3, 61.6, 61.2, 60.1, 58.8, 55.3 (10 s, PtC≡C*C*≡*CC*≡*CC*≡*CC*≡*CC*≡*C*), 21.4 (s, *C*H$_3$, *p* to P), 20.5 (s, *C*H$_3$, *p* to Pt), 7.3 (s, CH_2CH_3), 4.2 ppm (s, CH_2CH_3); $^{31}P\{^1H\}$ NMR ($CDCl_3$): δ = 19.0 ppm (s, ^1J(P,Pt) = 2891 Hz);[50] IR data: Table 2; UV/Vis data: Table 4; MS:[51] *m*/*z* (%): 1177 (1) **[$PtC_{14}Si$]$^+$**, 894 (34) [Pt(*p*-tol){P(*p*-tol)$_3$}$_2$]$^+$, 803 (100) [Pt{P(*p*-tol)$_3$}$_2$]$^+$), 497 (31) [Pt{P(*p*-tol)$_3$}]$^+$, 405 (44) [Pt{P(*p*-tol)$_2$}]$^+$.

***trans*,*trans*-[(*p*-tol){P(*p*-tol)$_3$}$_2$Pt(C≡C)$_3$Pt{P(*p*-tol)$_3$}$_2$(*p*-tol)] (PtC_6Pt)**

Method A: A Schlenk flask was charged with **PtC_6Si** (0.100 g, 0.0924 mmol) and THF (3 mL). Then wet nBu$_4$N$^+$F$^-$ (1.0 M in THF/5 wt% H_2O, 0.092 mL, 0.092 mmol) was added with stirring. After 0.5 h, the mixture was poured into a second Schlenk flask that had been charged with **PtCl** (0.214 g, 0.230 mmol), CuI (0.040 g, 0.22 mmol), and $HNEt_2$ (8 mL). The mixture was stirred for 65 h. The solvent was removed by rotary evaporation. The residue was extracted with toluene (4×25 mL). The combined extracts were passed through an alumina column (2×7 cm). The solvent was removed by rotary evaporation. The residue was suspended in hexane/EtOH (20 mL, 3:1 v/v), collected by filtration, and dried by oil pump vacuum to give **PtC_6Pt** as a yellow solid (0.096 g, 0.052 mmol, 56%).

Method B: A Schenk flask was charged with $Me_3Si(C{\equiv}C)_3SiMe_3$ (0.021 g, 0.10 mmol)[28] and THF (3 mL), and cooled to −78 °C (CO_2/acetone). Then wet nBu$_4$N$^+$F$^-$ (1.0 M in THF/5 wt% H_2O, 0.20 mL, 0.20 mmol) was added with stirring. After 0.5 h, the solution was added through a cannula to a Schlenk flask that had been charged with **PtCl** (0.223 g, 0.200 mmol), CuI (0.066 g, 0.35 mmol), and $HNEt_2$ (9 mL), and cooled to −45 °C. After 2 h, the cold bath was allowed to warm. After 60 h, the solvent was removed by rotary evaporation. The residue was extracted with toluene (3×35 mL). The extracts were filtered through an alumina column (2×7 cm). The solvent was removed by rotary evaporation. The residue was suspended in EtOH (15 mL), collected by filtration, and dried by oil pump vacuum to give **PtC_6Pt** as a yellow solid (0.056 g, 0.030 mmol, 30%). DSC/TGA data: Table 1; elemental analysis calcd (%) for $C_{104}H_{98}P_4Pt_2$: C 67.09, H 5.31; found: C 66.78, H 5.61; ^{1}H NMR ($CDCl_3$): δ = 7.32–7.28 (m, 24H; *o* to P), 6.95 (d, ^3J(H,H) = 8.3 Hz, 12H; *m* to P), 6.25 (d, ^3J(H,H) = 7.7 Hz, 4H; *o* to Pt), 5.97 (d, ^3J(H,H) = 7.7 Hz, 4H; *m* to Pt), 2.24 (s, 36H; CH_3), 1.90 ppm (s, 6H; CH_3); $^{13}C\{^1H\}$ NMR ($CDCl_3$): δ = 151.4 (t, ^2J(C,P) = 10.2 Hz, *i* to Pt), 139.4 (s, *p* to P), 139.1 (s, *o* to Pt), 134.7 (virtual t, ^2J(C,P) = 6.0 Hz, *o* to P),[20] 128.8 (s, *p* to Pt), 128.4 (virtual t, ^1J(C,P) = 29.2 Hz, *i* to P),[20] 127.8 (virtual t, ^3J(C,P) = 5.5 Hz, *m* to P),[20] 127.4 (s, *m* to Pt), 107.3 (t, ^2J(C,P) = 15.3 Hz, Pt*C*≡C), 99.4 (s, PtC≡*C*), 60.5 (s, PtC≡*CC*), 21.3 (s, *C*H$_3$, *p* to P), 20.5 ppm (s, *C*H$_3$, *p* to Pt); $^{31}P\{^1H\}$ NMR ($CDCl_3$): δ = 19.2 ppm (s, ^1J(P,Pt) = 2964 Hz);[50] IR data: Table 2; UV/Vis data: Table 4; MS:[51] *m*/*z* (%): 1860 (10) **[PtC_6Pt]$^+$**, 894 (74) [Pt(*p*-tol){P(*p*-tol)$_3$}$_2$]$^+$, 803 (100) [Pt{P(*p*-tol)$_3$}$_2$]$^+$, 497 (34) [Pt{P(*p*-tol)$_3$}]$^+$, 405 (44) [Pt{P(*p*-tol)$_2$}]$^+$.

***trans*,*trans*-[(*p*-tol){P(*p*-tol)$_3$}$_2$Pt(C≡C)$_4$Pt{P(*p*-tol)$_3$}$_2$(*p*-tol)] (PtC_8Pt)**: A three-necked flask was charged with **PtC_4H** (0.205 g, 0.217 mmol) and acetone (25 mL), and fitted with a gas dispersion tube and a condenser.[52] A Schlenk flask was charged with CuCl (0.090 g, 0.91 mmol), and TMEDA (0.050 mL, 0.33 mmol) was added with stirring. After 0.5 h, stirring was halted, and a grayish solid separated from a blue supernatant. Then O_2 was bubbled through the three-necked flask with stirring. After about 5 min, the solution was heated to 40 °C (oil bath) and the blue supernatant was added in portions. After 6 h, the solvent was removed by rotary evaporation. The residue was extracted with toluene (4×25 mL). The extracts were filtered through an alumina column (2×7 cm). The solvent was removed by rotary evaporation. The residue was suspended in MeOH (20 mL), collected by filtration, and dried by oil pump vacuum to give **PtC_8Pt** as a yellow solid (0.151 g, 0.080 mmol, 74%). DSC/TGA data: Table 1; elemental analysis calcd (%) for $C_{106}H_{98}P_4Pt_2$: C 67.51, H 5.24; found: C 67.26, H 5.28; ^{1}H NMR ($CDCl_3$): δ = 7.31–7.26 (m, 24H; *o* to P), 6.98 (d, ^3J(H,H) = 7.8 Hz, 12H; *m* to P), 6.25 (d, ^3J(H,H) = 7.8 Hz, 4H; *o* to Pt), 6.00 (d, ^3J(H,H) = 7.7 Hz, 4H; *m* to Pt), 2.29 (s, 36H; CH_3), 1.91 ppm (s, 6H; CH_3); $^{13}C\{^1H\}$ NMR ($CDCl_3$): δ = 150.7 (t, ^2J(C,P) = 10.2 Hz, *i* to Pt), 139.7 (s, *p* to P), 138.8 (s, *o* to Pt), 134.6 (virtual t, ^2J(C,P) = 6.0 Hz, *o* to P),[20] 129.1 (s, *p* to Pt), 128.3 (virtual t, ^3J(C,P) = 5.5 Hz, *m* to P),[20] 128.0 (virtual t, ^1J(C,P) = 29.6 Hz, *i* to P),[20] 127.6 (s, *m* to Pt), 112.9 (t, ^2J(C,P) = 15.7 Hz, PtC≡C), 97.6 (s, PtC≡*C*), 63.8 (s, PtC≡*C*C≡C), 57.7 (s, PtC≡CC≡*C*), 21.4 (s, *C*H$_3$, *p* to P), 20.6 ppm (s, *C*H$_3$, *p* to Pt); $^{31}P\{^1H\}$ NMR ($CDCl_3$): δ = 19.0 ppm (s, ^1J(P,Pt) = 2931 Hz);[50] IR data: Table 2; UV/Vis data: Table 4; MS:[51] *m*/*z* (%): 1860 (2) **[PtC_8Pt]$^+$**, 894 (54), [Pt(*p*-tol){P(*p*-tol)$_3$}$_2$]$^+$, 803 (100) [Pt{P(*p*-tol)$_3$}$_2$]$^+$.

***trans*,*trans*-[(*p*-tol){P(*p*-tol)$_3$}$_2$Pt(C≡C)$_5$Pt{P(*p*-tol)$_3$}$_2$(*p*-tol)] ($PtC_{10}Pt$)**: A Schlenk flask was charged with **$PtC_{10}Si$** (0.092 g, 0.081 mmol) and THF (5 mL), and cooled to 0 °C. Then wet nBu$_4$N$^+$F$^-$ (1.0 M in THF/5 wt% H_2O, 0.080 mL, 0.080 mmol) was added with stirring. After 0.5 h, the mixture was poured into a second Schlenk flask that had been charged with **PtCl** (0.127 g, 0.137 mmol), CuI (0.020 g, 0.11 mmol), and $HNEt_2$ (20 mL), and cooled to 0 °C. The mixture was stirred. After 4.5 h, the cold bath was removed and the solvent was removed by oil pump vacuum. The residue was extracted with toluene (4×25 mL). The combined extracts were passed through an alumina column (2×7 cm). The solvent was removed by rotary evaporation. The residue was suspended in MeOH (10 mL), collected by filtration, and dried by oil pump vacuum to give **$PtC_{10}Pt$** as an orange solid (0.130 g, 0.140 mmol, 84%). DSC/TGA data: Table 1; elemental analysis calcd (%) for $C_{118}H_{98}P_4Pt_2$: C 69.81, H 4.87; found: C 68.91, H 5.25; ^{1}H NMR ($CDCl_3$): δ = 7.31–7.26 (m, 24H; *o* to P), 7.00 (d, ^3J(H,H) = 7.7 Hz, 24H; *m* to P), 6.27 (d, ^3J(H,H) = 7.7 Hz, 2H; *o* to Pt), 6.05 (d, ^3J(H,H) = 7.7 Hz, 2H; *m* to Pt), 2.31 (s, 36H; CH_3), 1.93 ppm (s, 6H; CH_3); $^{13}C\{^1H\}$ NMR ($CDCl_3$): δ = 150.0 (t, ^2J(C,P) = 10.7 Hz, *i* to Pt), 140.0 (s, *p* to P), 138.8 (s, *o* to Pt), 134.5 (virtual t, ^2J(C,P) = 6.1 Hz, *o* to P),[20] 129.4 (s, *p* to Pt), 128.4 (virtual t, ^3J(C,P) = 5.3 Hz, *m* to P),[20] 127.8 (virtual t, ^1J(C,P) = 29.0 Hz, *i* to P),[20] 127.7 (s, *m* to Pt), 117.3 (t, ^2J(C,P) = 15.3 Hz, Pt*C*≡C), 96.5 (s, PtC≡*C*), 64.7, 61.6, 56.8 (3 s, PtC≡C*C*≡*CC*), 21.4 (s, *C*H$_3$, *p* to P), 20.5 ppm (s, *C*H$_3$, *p* to Pt); $^{31}P\{^1H\}$ NMR ($CDCl_3$): δ = 19.1 ppm (s, ^1J(P,Pt) = 2911 Hz);[50] IR data: Table 2; UV/Vis data: Table 4; MS:[51] *m*/*z* (%): 1019 (2) **[$PtC_{10}Pt$]$^+$**, 894 (58) [Pt(*p*-tol){P(*p*-tol)$_3$}$_2$]$^+$, 803 (100) [Pt{P(*p*-tol)$_3$}$_2$]$^+$.

***trans*,*trans*-[(*p*-tol){P(*p*-tol)$_3$}$_2$Pt(C≡C)$_6$Pt{P(*p*-tol)$_3$}$_2$(*p*-tol)] ($PtC_{12}Pt$)**

Method A: A three-necked flask was charged with **PtC_6H** (0.150 g, 0.155 mmol) and acetone (25 mL), and fitted with a gas dispersion tube and a condenser.[52] A Schlenk flask was charged with CuCl (0.050 g, 0.51 mmol) and acetone (20 mL), and TMEDA (0.030 mL, 0.20 mmol) was added with stirring. After 0.5 h, stirring was halted, and a grayish solid separated from a blue supernatant. Then O_2 was bubbled through the three-necked flask with stirring. After about 5 min, the blue supernatant was added in portions. After 1 h, the solvent was removed by rotary evaporation. The residue was extracted with toluene (4×25 mL). The extracts were filtered through an alumina column (2×7 cm). The solvent was removed by rotary evaporation. The residue was suspended in MeOH (15 mL), collected by filtration, and dried by oil pump vacuum to give **$PtC_{12}Pt$** as a bright orange powder (0.123 g, 0.064 mmol, 83%).

Method B: A three-necked flask was charged with **PtC_6Si** (0.216 g, 0.200 mmol) and acetone (40 mL), and fitted with a gas dispersion tube and a condenser.[52] A Schlenk flask was charged with CuCl (0.218 g, 0.222 mmol) and acetone (20 mL), and TMEDA (0.200 mL, 1.32 mmol) was added with stirring. After 0.5 h, stirring was halted, and a grayish solid separated from a blue supernatant. Then wet nBu$_4$N$^+$F$^-$ (1.0 M in THF/5 wt% H_2O, 0.050 mL, 0.050 mmol) was added to the three-necked flask with stirring. After 0.5 h (TLC showed no reactant remaining), $ClSiMe_3$ (0.025 mL, 0.200 mmol) was added. After 10 min, O_2 was bubbled through the mixture with stirring. After about 5 min, the blue supernatant was added in portions. After 1.5 h, the solvent was removed by

rotary evaporation. The residue was extracted with toluene (4×25 mL). The extract were filtered through an alumina column (2×7 cm). The solvent was removed by rotary evaporation. The residue was suspended in MeOH (15 mL), collected by filtration, and dried by oil pump vacuum to give **$PtC_{12}Pt$** as a bright orange powder (0.17 g, 0.088 mmol, 88%). DSC/TGA data: Table 1; elemental analysis calcd (%) for $C_{110}H_{98}P_4Pt_2$: C 68.31, H 5.31; found: C 67.67, H 5.12; ^{1}H NMR ($CDCl_3$): δ=7.32–7.27 (m, 24H; *o* to P), 7.02 (d, ^3J(H,H)=7.7 Hz, 24H; *m* to P), 6.29 (d, ^3J(H,H)=7.8 Hz, 2H; *o* to Pt), 6.08 (d, ^3J(H,H)=7.7 Hz, 2H; *m* to Pt), 2.32 (s, 36H; CH_3), 1.95 ppm (s, 6H; CH_3); ^{13}C{^{1}H} NMR ($CDCl_3$): δ= 149.7 (t, ^2J(C,P)=10.7 Hz, *i* to Pt), 140.0 (s, *p* to P), 138.7 (s, *o* to Pt), 134.5 (virtual t, ^2J(C,P)=6.1 Hz, *o* to P),[20] 129.5 (s, *p* to Pt), 128.4 (virtual t, ^3J(C,P)=4.6 Hz, *m* to P),[20] 127.74 (s, *m* to Pt), 127.65 (virtual t, ^1J(C,P)=29.8 Hz, *i* to P),[20] 120.1 (t, ^2J(C,P)=14.5 Hz, Pt*C*≡C), 96.0 (s, PtC≡*C*), 65.9, 63.2, 60.5, 56.1 (4 s, PtC≡C*C*≡*CC*≡*C*), 21.0 (s, *C*H$_3$, *p* to P), 20.5 ppm (s, *C*H$_3$, *p* to Pt); ^{31}P{^{1}H} NMR ($CDCl_3$): δ=19.0 ppm (s, ^1J(P,Pt)=2908 Hz);[50] IR data: Table 2; UV/Vis data: Table 4; MS:[51] *m*/*z* (%): 1934 (4) [**$PtC_{12}Pt$**]$^+$, 894 (64) [Pt(*p*-tol){P(*p*-tol)$_3$}$_2$]$^+$, 803 (100) [Pt{P(*p*-tol)$_3$}$_2$]$^+$.

***trans*,*trans*-[(*p*-tol){P(*p*-tol)$_3$}$_2$Pt(C≡C)$_8$Pt{P(*p*-tol)$_3$}$_2$(*p*-tol)] ($PtC_{16}Pt$)**: A three-necked flask was charged with **PtC_8Si** (0.125 g, 0.113 mmol) and acetone (20 mL), fitted with a gas dispersion tube and a condenser, and cooled to 0°C. A Schlenk flask was charged with CuCl (0.218 g, 0.222 mmol) and acetone (20 mL), and TMEDA (0.200 mL, 1.33 mmol) was added with stirring. After 0.5 h, stirring was halted, and a grayish solid separated from a blue supernatant. Then wet nBu$_4$N$^+$F$^-$ (1.0 M in THF/5 wt% H_2O, 0.05 mL, 0.05 mmol) was added to the three-necked flask with stirring. After 0.5 h (TLC showed no reactant remaining), $ClSiMe_3$ (0.025 mL, 0.200 mmol) was added. After 10 min, O_2 was bubbled through the mixture with stirring. After about 5 min, the blue supernatant was added in portions. After 1.5 h, the solvent was removed by rotary evaporation at ambient temperature. The residue was subjected to chromatography on a silica gel column (2.5×25 cm, 35:65 v/v CH_2Cl_2/hexane). The solvent was removed from the product-containing fraction by rotary evaporation and oil pump vacuum to give **$PtC_{16}Pt$** as red solid (0.078 g, 0.039 mmol, 70%). DSC/TGA data: Table 1; elemental analysis calcd (%) for $C_{114}H_{98}P_4Pt_2$: C 69.08, H 4.98; found: C 69.09, H 5.31; ^{1}H NMR ($CDCl_3$): δ=7.28–7.25 (m, 24H; *o* to P), 7.01 (d, ^3J(H,H)=7.7 Hz, 24H; *m* to P), 6.26 (d, ^3J(H,H)=7.7 Hz, 2H; *o* to Pt), 6.07 (d, ^3J(H,H)= 7.7 Hz, 2H; *m* to Pt), 2.31 (s, 36H; CH_3), 1.94 ppm (s, 6H; CH_3); ^{13}C{^{1}H} NMR ($CDCl_3$): δ=149.3 (t, ^2J(C,P)=9.9 Hz, *i* to Pt), 140.1 (s, *p* to P), 138.6 (s, *o* to Pt), 134.5 (virtual t, ^2J(C,P)=6.1 Hz, *o* to P),[20] 129.7 (s, *p* to Pt), 128.4 (virtual t, ^3J(C,P)=4.8 Hz, *m* to P),[20] 127.8 (s, *m* to Pt), 127.5 (virtual t, ^1J(C,P)=30.5 Hz, *i* to P),[20] 123.3 (t, ^2J(C,P)=14.5 Hz, Pt*C*≡C), 95.5 (s, PtC≡*C*), 67.1, 65.3, 63.2, 61.3, 59.5, 55.7 (6 s, PtC≡C*C*≡ *CC*≡*CC*≡*C*), 21.4 (s, *C*H$_3$, *p* to P), 20.5 ppm (s, *C*H$_3$, *p* to Pt); ^{31}P{^{1}H} NMR ($CDCl_3$): δ=19.7 ppm (s, ^1J(P,Pt)=2903 Hz);[50] IR data: Table 2; UV/Vis data: Table 4; MS:[51] *m*/*z* (%): 1105 (<1) [**$PtC_{16}Pt$**]$^+$, 894 (30) [Pt(*p*-tol){P(*p*-tol)$_3$}$_2$]$^+$, 803 (100) [Pt{P(*p*-tol)$_3$}$_2$]$^+$.

***trans*,*trans*-[(*p*-tol){P(*p*-tol)$_3$}$_2$Pt(C≡C)$_{10}$Pt{P(*p*-tol)$_3$}$_2$(*p*-tol)] ($PtC_{20}Pt$)**: A three-necked flask was charged with **$PtC_{10}Si$** (0.056 g, 0.050 mmol) and acetone (20 mL), fitted with a gas dispersion tube and a condenser, and cooled to −25°C. A Schlenk flask was charged with CuCl (0.200 g, 2.02 mmol) and acetone (20 mL), and TMEDA (0.200 mL, 1.33 mmol) was added with stirring. After 0.5 h, stirring was halted, and a grayish solid separated from a blue supernatant. Then wet nBu$_4$N$^+$F$^-$ (1.0 M in THF/5 wt% H_2O, 0.05 mL, 0.05 mmol) was added to the three-necked flask with stirring. After 20 min (TLC showed no reactant remaining), $ClSiMe_3$ (0.025 mL, 0.200 mmol) was added. After 10 min, O_2 was bubbled through the mixture with stirring and the blue supernatant was added in portions. After 1.5 h, the solvent was removed by rotary evaporation. The residue was subjected to chromatography on a silica gel column (2.5×25 cm, 35:65 v/v CH_2Cl_2/hexane). The solvent was removed from the product-containing fraction by rotary evaporation (ice bath) and oil pump vacuum to give **$PtC_{20}Pt$** as a red solid (0.037 g, 0.018 mmol, 72%). DSC/TGA data: Table 1; elemental analysis calcd (%) for $C_{118}H_{98}P_4Pt_2$: C 69.81, H 4.87; found: C 68.91, H 5.25; ^{1}H NMR ($CDCl_3$): δ=7.28–7.23 (m, 24H; *o* to P), 7.02 (d, ^3J(H,H)=7.7 Hz, 24H; *m* to P), 6.25 (d, ^3J(H,H)=7.8 Hz, 2H; *o* to Pt), 6.07 (d, ^3J(H,H)=7.7 Hz, 2H; *m* to Pt), 2.31 (s, 36H; CH_3), 1.93 ppm (s, 6H; CH_3); ^{13}C{^{1}H} NMR ($CDCl_3$): δ=149.1 (t, ^2J(C,P)=10.7 Hz, *i* to Pt), 139.9 (s, *p* to P), 138.5 (s, *o* to Pt), 134.3 (virtual t, ^2J(C,P)=6.4 Hz, *o* to P),[20] 129.6 (s, *p* to Pt), 128.3 (virtual t, ^3J(C,P)=5.5 Hz, *m* to P),[20] 127.7 (s, *m* to Pt), 127.4 (virtual t, ^1J(C,P)=29.4 Hz, *i* to P),[20] 123.1 (t, ^2J(C,P)=14.5 Hz, Pt*C*≡C), 95.2 (s, PtC≡*C*), 67.7, 66.4, 64.6, 63.2, 62.0, 60.6, 59.1, 55.6 (8 s, PtC≡C*C*≡ *CC*≡*CC*≡*CC*≡*C*), 21.5 (s, *C*H$_3$, *p* to P), 20.7 ppm (s, *C*H$_3$, *p* to Pt); ^{31}P{^{1}H} NMR ($CDCl_3$): δ=19.0 ppm (s, ^1J(P,Pt)=2889 Hz);[50] IR data: Table 2; UV/Vis data: Table 4; MS:[51] *m*/*z* (%): 2029 (<1) [**$PtC_{20}Pt$**]$^+$, 894 (60) [Pt(*p*-tol){P(*p*-tol)$_3$}$_2$]$^+$, 803 (100) [Pt{P(*p*-tol)$_3$}$_2$]$^+$.

***trans*,*trans*-[(*p*-tol){P(*p*-tol)$_3$}$_2$Pt(C≡C)$_{12}$Pt{P(*p*-tol)$_3$}$_2$(*p*-tol)] ($PtC_{24}Pt$)**: A three-necked flask was charged with **$PtC_{12}Si$** (0.154 g, 0.133 mmol) and acetone (10 mL), fitted with a gas dispersion tube and a condenser,[52] and cooled to 10°C. A Schlenk flask was charged with CuCl (0.440 g, 4.44 mmol) and acetone (5 mL), and TMEDA (0.800 mL, 5.36 mmol) was added with stirring. After 0.5 h, stirring was halted, and a grayish solid separated from a blue supernatant. Then O_2 was bubbled through the three-necked flask with stirring, and the blue supernatant was added in portions. After 7 h, the solvent was removed by rotary evaporation (ice bath). The residue was subjected to chromatography on a silica gel column at 10°C (3×25 cm, 25:75 v/v CH_2Cl_2/hexane). The solvent was removed from the reactant- and product-containing fractions by rotary evaporation (ice bath) and oil pump vacuum to give **$PtC_{12}Si$** as an orange solid (0.060, 0.052 mmol, 38%) and **$PtC_{24}Pt$** as a deep red solid (0.030 g, 0.014 mmol, 36%). When samples were heated in capillaries, there were no visually well-defined changes (melting, etc.) below 350°C. DSC/TGA data: Table 1; elemental analysis calcd (%) for $C_{122}H_{98}P_4Pt_2$: C 70.51, H 4.75; found: C 69.93, H 5.04; ^{1}H NMR ($CDCl_3$, 10°C): δ=7.32–7.21 (m, 24H; *o* to P), 6.97 (d, ^3J(H,H)=7.7 Hz, 24H; *m* to P), 6.23 (d, ^3J(H,H)= 7.7 Hz, 2H; *o* to Pt), 6.07 (d, ^3J(H,H)=7.7 Hz, 2H; *m* to Pt), 2.20 (s, 36H; CH_3), 1.88 ppm (s, 6H; CH_3); ^{13}C{^{1}H} NMR ($CDCl_3$, 10°C): δ= 149.0 ppm (s, *i* to Pt), 140.2 (s, *p* to P), 138.5 (s, *o* to Pt), 134.4 (virtual t, ^2J(C,P)=6.2 Hz, *o* to P),[20] 129.8 (s, *p* to Pt), 128.0 (virtual t, ^3J(C,P)= 5.5 Hz, *m* to P),[20] 127.8 (s, *m* to Pt), 127.2 (virtual t, ^1J(C,P)=29.6 Hz, *i* to P),[20] 125.6 (s, Pt*C*≡C), 95.0 (s, PtC≡*C*), 67.7, 66.6, 65.1, 64.0, 63.1, 62.2, 61.3, 60.1, 58.8, 55.3 (10 s, PtC≡C*C*≡*CC*≡*CC*≡*CC*≡*CC*≡*C*), 21.5 (s, *C*H$_3$, *p* to P), 20.5 ppm (s, *C*H$_3$, *p* to Pt); ^{31}P{^{1}H} NMR ($CDCl_3$, 10°C): δ=19.7 ppm (s, ^1J(P,Pt)=2886 Hz);[50] IR data: Table 2; UV/Vis data: Table 4; MS:[51] *m*/*z* (%): 2078 (<1) [**$PtC_{24}Pt$**]$^+$, 894 (52) [Pt(*p*-tol){P(*p*-tol)$_3$}$_2$]$^+$, 803 (100) [Pt{P(*p*-tol)$_3$}$_2$]$^+$.

***trans*,*trans*-[(*p*-tol){P(*p*-tol)$_3$}$_2$Pt(C≡C)$_{14}$Pt{P(*p*-tol)$_3$}$_2$(*p*-tol)] ($PtC_{28}Pt$)**: A three-necked flask was charged with **$PtC_{14}Si$** (0.50 g, 0.42 mmol) and acetone (15 mL), fitted with a gas dispersion tube and a condenser,[52] and cooled to 0°C. A Schlenk flask was charged with CuCl (0.440 g, 4.44 mmol) and acetone (5 mL), and TMEDA (0.800 mL, 5.36 mmol) was added with stirring. After 0.5 h, stirring was halted, and a grayish solid separated from a blue supernatant. Then O_2 was bubbled through the three-necked flask with stirring, and the blue supernatant was added in portions. After 42 h, acetone (10 mL, 0°C) was added. After another 16 h, the solvent was removed by rotary evaporation (ice bath). The residue was subjected to chromatography on a silica gel column (3×25 cm, 25:75 v/v CH_2Cl_2/hexane). The solvent was removed from the product-containing fraction by rotary evaporation (ice bath) and oil pump vacuum to give **$PtC_{28}Pt$** as a deep red solid (0.023 g, 0.021 mmol, 51%). When samples were heated in capillaries, there were no visually well-defined changes (melting, etc.) below 350°C. DSC/TGA data: Table 1; elemental analysis calcd (%) for $C_{126}H_{98}P_4Pt_2$: C 71.18, H 4.65; found: C 69.82, H 4.94; ^{1}H NMR ($CDCl_3$, 0°C): δ=7.30–7.26 (m, 24H; *o* to P), 7.07 (d, ^3J(H,H)=7.6 Hz, 24H; *m* to P), 6.25 (d, ^3J(H,H)=7.7 Hz, 2H; *o* to Pt), 6.07 (d, ^3J(H,H)=7.5 Hz, 2H; *m* to Pt), 2.31 (s, 36H; CH_3), 1.98 ppm (s, 6H; CH_3); ^{13}C{^{1}H} NMR ($CDCl_3$, 0°C): δ=148.9 (t, ^2J-(C,P)=10.2 Hz, *i* to Pt), 140.1 (s, *p* to P), 138.5 (s, *o* to Pt), 134.4 (virtual t, ^2J(C,P)=6.2 Hz, *o* to P),[20] 129.8 (s, *p* to Pt), 128.0 (virtual t, ^3J(C,P)= 5.5 Hz, *m* to P),[20] 127.8 (s, *m* to Pt), 127.2 (virtual t, ^1J(C,P)=30.4 Hz, *i* to P),[20] 126.0 (s, Pt*C*≡C), 95.0 (s, PtC≡*C*), 67.9, 66.9, 65.4, 64.5, 63.7, 63.1, 62.5, 61.8, 61.0, 60.0, 58.8, 55.3 (12 s, PtC≡C*C*≡*CC*≡*CC*≡*CC*≡*CC*≡ *CC*≡*C*), 21.4 (s, *C*H$_3$, *p* to P), 20.6 ppm (s, *C*H$_3$, *p* to Pt); ^{31}P{^{1}H} NMR ($CDCl_3$, 0°C): δ=19.7 ppm (s, ^1J(P,Pt)=2885 Hz);[50] IR data: Table 2;

UV/Vis data: Table 4; MS:[51] *m/z* (%): 2125 (<1) $[\mathbf{PtC_{28}Pt}]^+$, 894 (43) $[Pt(p\text{-tol})\{P(p\text{-tol})_3\}_2]^+$, 803 (100) $[Pt\{P(p\text{-tol})_3\}_2]^+$.

$H(C\equiv C)_2SiEt_3$:[24] A three-necked flask was fitted with a condenser and a dropping funnel, charged with a solution of $H(C\equiv C)_2H$ (5.38 g, 107 mmol) in THF (50 mL),[21] and cooled to −78 °C. Then *n*BuLi (1.6 M in hexane, 75.0 mL, 120 mmol) was added dropwise over 20 min with stirring. After 1 h, the cold bath was removed and $ClSiEt_3$ (18.0 g, 119 mmol) was added. After 3 h, cold saturated aqueous NH_4Cl (50 mL) was added. The mixture was extracted with pentane (3×100 mL). The combined extracts were dried (Na_2SO_4). The solvent was removed by rotary evaporation at ambient temperature. The residue was distilled by oil pump vacuum to give $H(C\equiv C)_2SiEt_3$ (33–38 °C, 2.3×10^{-2} mbar) as a colorless liquid (8.09 g, 49.2 mmol, 46%) and $Et_3Si(C\equiv C)_2SiEt_3$ (137–143 °C, 2.3×10^{-2} mbar) as a pale yellow liquid (11.9 g, 42.7 mmol, 40%).[24a] ^1H NMR ($CDCl_3$): $\delta=1.97$ (s, 1H; HC≡), 0.90 (t, $^3J(H,H)=7.8$ Hz, 9H; CH_3), 0.56 ppm (q, $^3J(H,H)=7.8$ Hz, 6H; CH_2); $^{13}C\{^1H\}$ NMR ($CDCl_3$): $\delta=88.7$ (s, *C*≡CSi), 83.2 (s, C≡*C*Si), 68.8 (s, HC≡*C*), 66.3 (s, H*C*≡C), 7.7 (s, *C*H_3), 4.4 ppm (s, *C*H_2); IR (liquid film): $\tilde{\nu}=3308$ (m, $\nu_{\equiv C-H}$), 2189/2034 cm^{-1} (w/m, $\nu_{C\equiv C}$).

Cyclic voltammetry: A BAS CV-50W Voltammetric Analyzer (Cell Stand C3) with the program CV-50W (version 2.0) was employed. Cells were fitted with Pt working and counter electrodes, and a Ag wire pseudoreference electrode. All sample solutions (CH_2Cl_2) were $5–10\times10^{-3}$ M in substrate and 0.1 M in $nBu_4N^+BF_4^-$ (crystallized from ethanol/hexane and dried by oil pump vacuum), and were prepared under nitrogen. Ferrocene was subsequently added (0.46 V), and calibration voltammograms recorded. The ambient laboratory temperature was 22.5±1 °C.

Crystallography

Procedure for PtC_6Si: A solution of **PtC_6Si** in $ClCH_2CH_2Cl$ was layered with MeOH and kept in a refrigerator (−24 °C). After two days, the light yellow prisms were used for data collection as outlined in Table 5. Cell parameters were obtained from 10 frames using a 10° scan and refined with 11851 reflections. Lorentz, polarization, and absorption corrections[53] were applied. The space group was determined from systematic absences and subsequent least-squares refinement. The structure was solved by direct methods. The parameters were refined with all data by full-matrix least-squares on F^2 using SHELXL-97.[54] Non-hydrogen atoms were refined with anisotropic thermal parameters. The hydrogen atoms were fixed in idealized positions using a riding model. Scattering factors were taken from literature.[55]

Procedure for PtC_8Si: Yellow prisms of **PtC_8Si** were grown from layered CH_2Cl_2/MeOH (−24 °C, 2 d) and analyzed as described for **PtC_6Si** (cell parameters from 10 frames using a 10° scan; refined with 12866 reflections). The structure was solved and refined as with **PtC_6Si**. The unit cell contained four molecules of CH_2Cl_2.

Procedure for $PtC_{10}Si$: Yellow prisms of **$PtC_{10}Si$** were grown and analyzed as described for **PtC_8Si** (cell parameters from 10 frames using a 10° scan; refined with 9258 reflections). The structure was solved and refined as with **PtC_6Si**.

Procedure for PtC_6Pt: A solution of **PtC_6Pt** in benzene was taken to apparent dryness by oil pump vacuum, and the residue was dissolved in toluene and layered with MeOH. After one week (room temperature), the light yellow prisms were analyzed as described for **PtC_6Si** (cell parameters from 10 frames using a 10° scan; refined with 10505 reflections). The structure was solved and refined as with **PtC_6Si**. The structure exhibited an inversion center at the midpoint of the C3−C3a bond. The unit cell contained two molecules of benzene.

Procedure for $PtC_{10}Pt$: A solution of **$PtC_{10}Pt$** in benzene was layered with EtOH. After two days (room temperature), the orange prisms were analyzed as described for **PtC_6Si** (cell parameters from 10 frames using a 10° scan; refined with 10097 reflections). The structure was solved and refined as with **PtC_6Si**, and exhibited an inversion center at the midpoint of the C5−C5a bond.

Procedure for $Pt'C_8Pt'$: Acetone vapor was allowed to diffuse into a solution of **$Pt'C_8Pt'$** (the primes denote PPh_3 in place of the $P(p\text{-tol})_3$ ligands) in 1,2-difluorobenzene.[15a] After two weeks (room temperature), the thin pale yellow plates were used for data collection as outlined in Table 5. Cell parameters were obtained from 10 frames using a 10° scan. The space group was determined from systematic absences and least-squares refinement. Lorentz, polarization, and absorption corrections were applied.[56] The structure was solved by standard heavy atom techniques and refined with SHELXTL. Non-hydrogen atoms were refined with anisotropic thermal parameters. The structure exhibited an inversion center at the midpoint of the C4−C4a bond. The unit cell contained four disordered molecules of acetone and a half molecule of 1,2-difluorobenzene. Hydrogen atom positions were fixed in idealized positions using a riding model. Scattering factors and $\Delta f'$ and $\Delta f''$ values were taken from literature.[57,58]

Procedure for $PtC_{12}Pt$: A solution of **$PtC_{12}Pt$** in benzene was layered with EtOH. After one week (room temperature), pale yellow prisms were analyzed as described for **$Pt'C_8Pt'$** (cell parameters from 10 frames using a 10° scan). The structure was solved and refined similarly to **$Pt'C_8Pt'$**, except for the software employed (SIR 97),[59] and exhibited an inversion center at the midpoint of the C6−C6a bond. The unit cell contained two molecules of benzene.

CCDC-606021 (**PtC_6Si**), CCDC-606020 (**PtC_8Si**·(CH_2Cl_2)), CCDC-606019 (**$PtC_{10}Si$**), CCDC-606018 (**PtC_6Pt**·(benzene)$_2$), CCDC-124681 (**$Pt'C_8Pt'$**·(acetone)$_4$·(1,2-difluorobenzene)$_{0.5}$), CCDC-606022 (**$PtC_{10}Pt$**), and CCDC-124885 (**$PtC_{12}Pt$**·(benzene)$_2$) contain the supplementary crystallographic data for this paper. These data can be obtained free of charge from The Cambridge Crystallographic Data Centre via www.ccdc.cam.ac.uk/data_request/cif.

Acknowledgements

We thank the Deutsche Forschungsgemeinschaft (DFG, GL 300/1–3) and US NSF (CHE-9732605) for support, and Dr. Atta Arif for the crystal structures of **$Pt'C_8Pt'$** and **$PtC_{12}Pt$**.[15a]

[1] *Acetylene Chemistry* (Eds.: F. Diederich, P. J. Stang, R. Tykwinski) Wiley-VCH, Weinheim, **2004**, and earlier volumes in this series.
[2] M. I. Bruce, P. J. Low, *Adv. Organomet. Chem.* **2004**, *50*, 179.
[3] F. Paul, C. Lapinte in *Unusual Structures and Physical Properties in Organometallic Chemistry* (Eds.: M. Gielen, R. Willem, B. Wrackmeyer) Wiley, New York, **2002**, pp. 220–291.
[4] S. Szafert, J. A. Gladysz, *Chem. Rev.* **2003**, *103*, 4175.
[5] N. J. Long, C. K. Williams, *Angew. Chem.* **2003**, *115*, 2690; *Angew. Chem. Int. Ed.* **2003**, *42*, 2586.
[6] Representative papers since the review in reference [3]: a) M. I. Bruce, B. G. Ellis, P. J. Low, B. W. Skelton, A. H. White, *Organometallics* **2003**, *22*, 3184; b) H. Jiao, K. Costuas, J. A. Gladysz, J.-F. Halet, M. Guillemot, L. Toupet, F. Paul, C. J. Lapinte, *J. Am. Chem. Soc.* **2003**, *125*, 9511; c) S. Kheradmandan, K. Venkatesan, O. Blacque, H. W. Schmalle, H. Berke, *Chem. Eur. J.* **2004**, *10*, 4872, and earlier work cited therein.
[7] a) Y. Tobe, T. Wakabayashi in *Acetylene Chemistry* (Eds.: F. Diederich, P. J. Stang, R. Tykwinski) Wiley-VCH, Weinheim, **2004**, Chapter 9; b) *Polyynes: Synthesis, Properties and Applications*, (Ed.: F. Cataldo) Taylor & Francis, New York, **2005**.
[8] T. Bartik, W. Weng, J. A. Ramsden, S. Szafert, S. B. Falloon, A. M. Arif, J. A. Gladysz, *J. Am. Chem. Soc.* **1998**, *120*, 11071.
[9] a) $FeC_{12}Fe$ and FeC_6Fe complexes: A. Sakurai, M. Akita, Y. Moro-oka, *Organometallics* **1999**, *18*, 3241; b) FeC_8Fe and FeC_4Fe complexes: M. Akita, M.-C. Chung, A. Sakurai, S. Sugimoto, M. Terada, M. Tanaka, Y. Moro-oka, *Organometallics* **1997**, *16*, 4882.
[10] a) $RuC_{14}Ru$ complex: A. B. Antonova, M. I. Bruce, B. G. Ellis, M. Gaudio, P. A. Humphrey, M. Jevric, G. Melino, B. K. Nicholson, G. J. Perkins, B. W. Skelton, B. Stapleton, A. H. White, N. N. Zaitseva, *Chem. Commun.* **2004**, 960; b) $RuC_{12}Ru$ complex: S. Rigaut, J. Perruchon, L. Le Pichon, D. Touchard, P. H. Dixneuf, *J. Organomet. Chem.* **2003**, *670*, 37; c) $RuC_{12}Ru$ complex: H. Qi, A. Gupta, B. C. Noll, G. L. Snider, Y. Lu, C. Lent, T. P. Fehlner, *J. Am. Chem. Soc.* **2005**, *127*, 15218; d) RuC_8Ru and RuC_6Ru complexes: M. I. Bruce,

B. D. Kelly, B. W. Skelton, A. H. White, *J. Organomet. Chem.* **2000**, *604*, 150, and references therein; e) RuC_4Ru complex: M. I. Bruce, P. J. Low, K. Costuas, J.-F. Halet, S. P. Best, G. A. Heath, *J. Am. Chem. Soc.* **2000**, *122*, 1949; f) see also M. I. Bruce, B. G. Ellis, P. J. Low, B. W. Skelton, A. H. White, *Organometallics* **2003**, *22*, 3184.

[11] a) $ReC_{20}Re$, $ReC_{16}Re$, $ReC_{12}Re$, $ReC_{10}Re$, ReC_8Re, and ReC_6Re complexes: R. Dembinski, T. Bartik, B. Bartik, M. Jaeger, J. A. Gladysz, *J. Am. Chem. Soc.* **2000**, *122*, 810; b) ReC_4Re complexes: M. Brady, W. Weng, Y. Zhou, J. W. Seyler, A. J. Amoroso, A. M. Arif, M. Böhme, G. Frenking, J. A. Gladysz, *J. Am. Chem. Soc.* **1997**, *119*, 775; c) W. E. Meyer, A. J. Amoroso, C. R. Horn, M. Jaeger, J. A. Gladysz, *Organometallics* **2001**, *20*, 1115; d) C. R. Horn, J. M. Martín-Alvarez, J. A. Gladysz, *Organometallics* **2002**, *21*, 5386; e) C. R. Horn, J. A. Gladysz, *Eur. J. Inorg. Chem.* **2003**, *9*, 2211.

[12] $RhC_{12}Rh$ complex: G.-Y. Xu, G. Zou, Y.-H. Ni, M. C. DeRosa, R. J. Crutchley, T. Ren, *J. Am. Chem. Soc.* **2003**, *125*, 10057.

[13] $PtC_{16}Pt$, $PtC_{12}Pt$, PtC_8Pt, PtC_6Pt, and PtC_4Pt complexes: W. Mohr, J. Stahl, F. Hampel, J. A. Gladysz, *Chem. Eur. J.* **2003**, *9*, 3324.

[14] $PtC_{12}Pt$, PtC_8Pt, and PtC_6Pt complexes: a) J. Stahl, J. C. Bohling, E. B. Bauer, T. B. Peters, W. Mohr, J. M. Martín-Alvarez, F. Hampel, J. A. Gladysz, *Angew. Chem.* **2002**, *114*, 1951; *Angew. Chem. Int. Ed.* **2002**, *41*, 1871; b) G. R. Owen, J. Stahl, F. Hampel, J. A. Gladysz, *Organometallics* **2004**, *23*, 5889; c) L. de Quadras, F. Hampel, J. A. Gladysz, *Dalton Trans.* **2006**, 2929.

[15] a) T. B. Peters, J. C. Bohling, A. M. Arif, J. A. Gladysz, *Organometallics* **1999**, *18*, 3261; b) Q. Zheng, J. A. Gladysz, *J. Am. Chem. Soc.* **2005**, *127*, 10508.

[16] a) K. Sonogashira, Y. Fujikura, N. Toyoshima, S. Takahashi, N. Hagihara, *J. Organomet. Chem.* **1978**, *145*, 101; b) M. I. Bruce, M. Ke, P. J. Low, *Chem. Commun.* **1996**, 2405; c) S. M. AlQaisi, K. J. Galat, M. Chai, D. G. Ray III, P. L. Rinaldi, C. A. Tessier, W. J. Youngs, *J. Am. Chem. Soc.* **1998**, *120*, 12149.

[17] H. C. Clark, L. E. Manzer, *J. Organomet. Chem.* **1973**, *59*, 411.

[18] Previous characterization via an alternative synthesis: C. Eaborn, K. J. Odell, A. Pidcock, *J. Chem. Soc. Dalton Trans.* **1978**, 357.

[19] Previous characterization via an alternative synthesis: J. Ertl, D. Grafl, H. A. Brune, *Z. Naturforsch. B* **1982**, *37*, 1082.

[20] W. H. Hersh, *J. Chem. Educ.* **1997**, *74*, 1485.

[21] a) L. Brandsma, H. D. Verkruijsse, *Synth. Commun.* **1991**, *21*, 657; b) L. Brandsma, H. D. Verkruijsse, *Synthesis of Acetylenes, Allenes and Cumulenes*, Elsevier, New York, **1981**, p. 136 and p. 146. The HC≡CC≡CH concentration is calculated from the mass increase of the THF. This compound is reported to be explosive.

[22] P. Siemsen, R. C. Livingston, F. Diederich, *Angew. Chem.* **2000**, *112*, 2740; *Angew. Chem. Int. Ed.* **2000**, *39*, 2632; .

[23] R. Eastmond, T. R. Johnson, D. R. M. Walton, *J. Organomet. Chem.* **1973**, *50*, 87.

[24] a) R. Eastmond, T. R. Johnson, D. R. M. Walton, *Tetrahedron* **1972**, *28*, 4601; b) For an alternative synthesis, see reference [11a].

[25] For additional details, see Q. Zheng, Doctoral Thesis, Universität Erlangen-Nürnberg, **2005**.

[26] J. C. Bohling, T. B. Peters, A. M. Arif, F. Hampel, J. A. Gladysz, in *Coordination Chemistry at the Turn of the Century* (Eds.: G. Ondrejovic, A. Sirota), Slovak Technical University Press, Bratislava, Slovokia, **1999**, pp. 47–52.

[27] For a conceptually related approach to Eglinton couplings of terminal alkynes, see M. M. Haley, M. L. Bell, S. C. Brand, D. B. Kimball, J. J. Pak, W. B. Wan, *Tetrahedron Lett.* **97**, *38*, 7483.

[28] Y. Rubin, S. S. Lin, C. B. Knobler, J. Anthony, A. M. Boldi, F. Diederich, *J. Am. Chem. Soc.* **1991**, *113*, 6943.

[29] W. Weng, T. Bartik, M. Brady, B. Bartik, J. A. Ramsden, A. M. Arif, J. A. Gladysz, *J. Am. Chem. Soc.* **1995**, *117*, 11922.

[30] For additional details, see A. Frisch, Diplom Thesis, Universität Erlangen-Nürnberg, **1999**.

[31] DSC and TGA data were treated as recommended by H. K. Cammenga, M. Epple, *Angew. Chem.* **1995**, *107*, 1284; *Angew. Chem. Int. Ed. Engl.* **1995**, *34*, 1171. The T_e values best represent the temperature of the phase transition or exotherm. DSC measurements were generally not continued above the initial mass loss temperature (TGA).

[32] F. Zhuravlev, J. A. Gladysz, *Chem. Eur. J.* **2004**, *10*, 6510.

[33] The analogous pentafluorophenyl complexes exhibit no reductions prior to the CH_2Cl_2-induced limit.[13] Therefore the more electron rich complexes **PtC_xPt** are presumed to be similarly unreactive.

[34] a) T. Luu, E. Elliot, A. D. Slepkov, S. Eisler, R. McDonald, F. A. Hegmann, R. R. Tykwinski, *Org. Lett.* **2005**, *7*, 51; b) S. Eisler, A. D. Slepkov, E. Elliot, T. Luu, R. McDonald, F. A. Hegmann, R. R. Tykwinski, *J. Am. Chem. Soc.* **2005**, *127*, 2666.

[35] L. Blanco, H. E. Helson, M. Hirthammer, H. Mestdagh, S. Spyroudis, K. P. C. Vollhardt, C. *Angew. Chem.* **1987**, *99*, 1276; *Angew. Chem. Int. Ed. Engl.* **1987**, *26*, 1246; .

[36] D. W. Rogers, A. A. Zavitsas, N. Matsunaga, *J. Phys. Chem. A* **2005**, *109*, 9169 (see Supporting Information).

[37] For a lead reference to an extensive literature, see J. Xiao, M. Yang, J. W. Lauher, F. W. Fowler, *Angew. Chem.* **2000**, *112*, 2216; *Angew. Chem. Int. Ed.* **2000**, *39*, 2132; .

[38] a) E. R. H. Jones, H. H. Lee, M. C. Whiting, *J. Chem. Soc.* **1960**, 3483; b) T. R. Johnson, D. R. M. Walton, *Tetrahedron* **1972**, *28*, 5221.

[39] T. Gibtner, F. Hampel, J.-P. Gisselbrecht, A. Hirsch, *Chem. Eur. J.* **2002**, *8*, 408.

[40] a) A. Klein, S. Hasenzahl, W. Kaim, J. Fiedler, *Organometallics* **1998**, *17*, 3532; b) M. Younus, A. Köhler, S. Cron, N. Chawdhury, M. R. A. Al-Mandhary, M. S. Khan, J. Lewis, N. J. Long, R. H. Friend, P. R. Raithby, *Angew. Chem.* **1998**, *110*, 3180; *Angew. Chem. Int. Ed.* **1998**, *37*, 3036; .

[41] Ľ. Horný, N. D. K. Petraco, C. Pak, H. F. Schaefer III, *J. Am. Chem. Soc.* **2002**, *124*, 5861.

[42] D. P. Arnold, M. A. Bennett, *Inorg. Chem.* **1984**, *23*, 2117.

[43] a) G. Schermann, T. Grösser, F. Hampel, A. Hirsch, *Chem. Eur. J.* **1997**, *3*, 1105; b) C. Klinger, O. Vostrowsky, A. Hirsch, *Eur. J. Org. Chem.* **2006**, 1508.

[44] A. D. Slepkov, F. A. Hegmann, S. Eisler, E. Elliot, R. R. Tykwinski, *J. Chem. Phys.* **2004**, *120*, 6807.

[45] The increase in intensities of these bands (e.g., from $\varepsilon = 361000$ to $402000\ M^{-1}\,cm^{-1}$ for **$PtC_{12}Pt$** vs. **$PtC_{28}Pt$**) is not as great as might have been expected from previous studies.[11,13a] However, a substantial increase in breadth and hence band area is evident in Figure 1.

[46] H. H. Jaffé, M. Orchin, *Theory and Applications of Ultraviolet Spectroscopy*, Wiley, New York, 1962; Table 11.7 and accompanying discussion.

[47] H. Meier, *Angew. Chem.* **2005**, *117*, 2536; *Angew. Chem. Int. Ed.* **2005**, *44*, 2482.

[48] W. Mohr, T. B. Peters, J. C. Bohling, F. Hampel, A. M. Arif, J. A. Gladysz, *Comptes Rendus Chemie* **2002**, *5*, 111.

[49] a) G. R. Owen, F. Hampel, J. A. Gladysz, *Organometallics* **2004**, *23*, 5893; b) Q. Zheng, F. Hampel, J. A. Gladysz, *Organometallics* **2004**, *23*, 5896.

[50] This coupling represents a satellite (d; $^{195}Pt = 33.8\,\%$), and is not reflected in the peak multiplicity given.

[51] Most intense peak of isotope envelope.

[52] In order to avoid the aspiration/volatilization of acetone, an efficient condenser is required.

[53] a) "Collect" data collection software, B. V. Nonius, **1998**; b) "Scalepack" data processing software: Z. Otwinowski, W. Minor, *Methods Enzymol.* **1997**, *276*, 307.

[54] G. M. Sheldrick, SHELX-97, Program for refinement of crystal structures, University of Göttingen, Göttingen (Germany), **1997**.

[55] D. T. Cromer, J. T. Waber, in *International Tables for X-ray Crystallography* (Eds.: J. A. Ibers, W. C. Hamilton), Kynoch, Birmingham (England), **1974**.

[56] G. M. Sheldrick, "SADABS: Area-Detector Absorption Correction", Siemens Industrial Automation, Inc., Madison, WI, **1996**.

[57] E. N. Maslen, A. G. Fox, M. A. O'Keefe, In *International Tables for Crystallography: Mathematical, Physical and Chemical Tables, Vol. C* (Ed.: A. J. C. Wilson), Kluwer, Dordrecht (The Netherlands), **1992**, Chapter 6, pp. 476–516.

[58] D. C. Creagh, W. J. McAuley, In *International Tables for Crystallography: Mathematical, Physical and Chemical Tables, Vol. C* (Ed.: A. J. C. Wilson), Kluwer, Dordrecht (The Netherlands), **1992**, Chapter 4, pp. 206–222.

[59] A. Altomare, M. C. Burla, M. Camalli, G. Cascarano, C. Giacovazzo, A. Guagliardi, A. G. G. Moliteni, G. Polidori, R. Spagna, *J. Appl. Crystallogr.* **1999**, *32*, 115.

Received: May 2, 2006
Published online: July 28, 2006

